Demulsifying Water-in-Bitumen Emulsions of Oil Sands Froth Treatment

by

Liang Chen

A thesis submitted in partial fulfillment of the requirements for the degree of

Master of Science

in

Chemical Engineering

Department of Chemical and Materials Engineering
University of Alberta

Abstract

The formation of stable water-in-oil emulsions during bitumen extraction poses problems for water separation from diluted bitumen, which leads to equipment corrosion and catalyst fouling in downstream operations. Demulsifiers are used to break the stable emulsions and assist the separation of water from diluted bitumen.

To study the factors influencing demulsification, the efficiency of four industrial demulsifiers in dewatering of water-in-toluene diluted bitumen emulsions was probed at various temperatures. The ability of the demulsifiers to compete for the interface was assessed by measuring interfacial tension of the toluene diluted bitumen-water interface in the presence and absence of demulsifiers. Demulsification tests were conducted using two different methods. A dynamic method was used to allow in-situ and real-time observation of the demulsification process. A static method was used to probe water removal efficiency of the four demulsifiers by gravity to assist the understanding of the demulsifiers' performance. In order to understand the impact of temperature on demulsification, the effect of temperature on the viscosity of the diluted bitumen was investigated and correlated to demulsification efficiency.

Acknowledgement

I would like to express my gratitude to my supervisor Dr. Zhenghe Xu whose decision to recruit me has allowed me to explore much in my own area. The unforgettable experience I gained while pursuing this degree will be cherished for life-long time.

Dr. David Harbottle and Dr. Erica Pensini provided uncountable suggestions and encouragements throughout my program. They have my sincere thanks for the guidance I received.

Thank you to Mr. James Skwarok, Ms. Jie Ru and Ms. Lisa Carreiro for their diligent work to maintain our great labs. I would not have achieved what I have without their efforts.

To many others who helped and inspired me during this period of time: May your beautiful souls be blessed.

Table of Contents

List of Tables

List of Figures

Chapter 1 Introduction

1.1 Oil sands processing and the origin of highly stable W/O emulsions in oil sands froth treatment

The discovery of bituminous oil sands in Alberta reshaped the global energy map. With 315 billion barrels of recoverable bitumen underground, Alberta oil reserves are comparable to the conventional oil reserves of Saudi Arabia [1]. By 2011, crude bitumen production of Alberta has reached over 1.7 million barrels per day (bbl/d). It is estimated that by 2021, crude bitumen production will be 3.7 million bbl/d [2]. Oil sands production, along with gas production and mining contribute more than a quarter of Alberta's gross domestic product (GDP). Problems related to bitumen recovery are of great concerns.

1.1.1 Bitumen extraction from oil sands

Oil sands are unconsolidated sand deposits that are impregnated with highly viscous petroleum, referred to as bitumen [3]. To extract bitumen from oil sands ore two types of strategies can be applied, depending on the reservoirs' characteristics. Open-pit mining allows bitumen enriched sands to be collected from relatively shallow oil sands formations (no deeper than 75 m) [4]. In-situ production techniques including Steam Assisted Gravity Drainage (SAGD) and Cyclical Steam Simulation (CSS) are used to recover bitumen where open-pit mining is not economical. Currently in Alberta more than half of bitumen production is through open-pit mining, with the rest being recovered by in-situ technologies [5].

Bitumen entrained with oil sands ore can be recovered using the hot water extraction technique. Figure 1.1.1 outlines the major operations involved in the hot water bitumen extraction process.

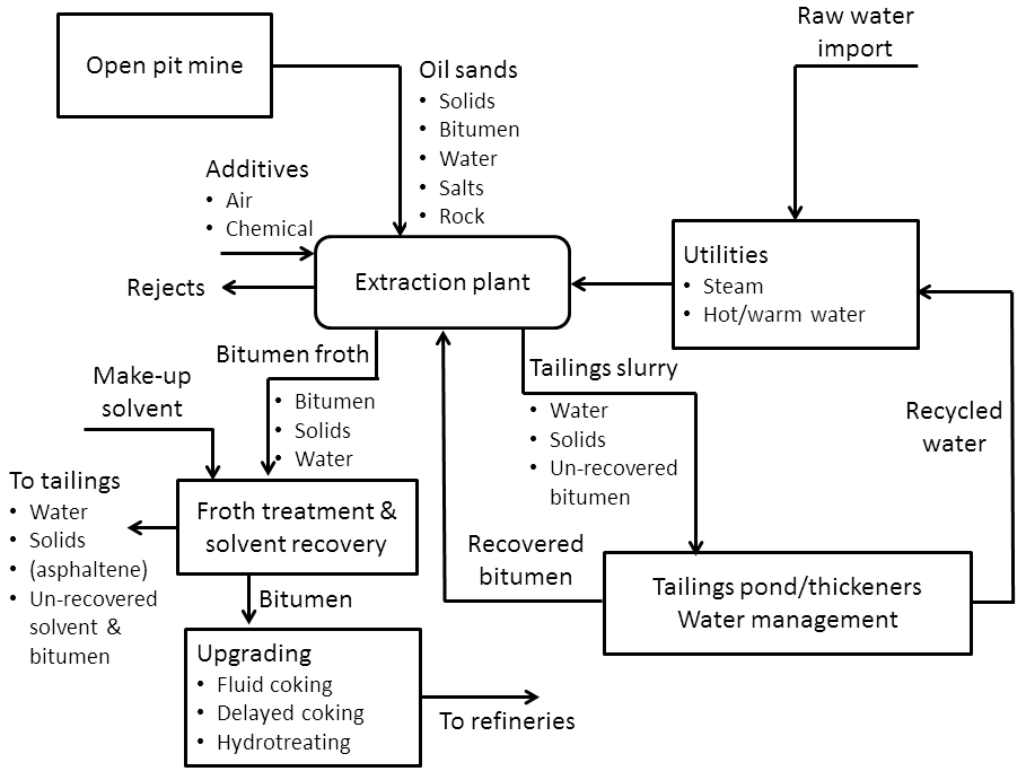

Figure 1.1.1 Bitumen extraction from oil sands ore. [3]

As shown in Figure 1.1.1, mined oil sands lumps are crushed and mixed with hot water, and then sent to extraction plant to initiate bitumen liberation. In the extraction plant liberated bitumen droplets attach to air bubbles and subsequently rise to the top of the separation vessel. The oil-rich phase that is skimmed off from the top of the separation vessel is known as primary bitumen froth. Typically after removing the entrained air, bitumen froth contains about 60 wt% bitumen, 30 wt% water and 10 wt% solids [6].

1.1.2 The origin of highly stable emulsion in bitumen froth treatment

After de-aeration, bitumen froth is sent to a froth treatment plant to remove remaining solids and water. The remaining water is mainly free water [6]. To initiate water-oil separation, light solvents are mixed with bitumen froth in order to reduce the density and viscosity of the oil phase. Currently there are two main variants of the froth treatment operations, namely naphthenic froth treatment and paraffinic froth treatment.

Heavy naphtha used in naphthenic froth treatment contains a wide range of materials from short-chain alkanes to aromatic hydrocarbons [7], whereas paraffinic solvents used in froth treatment are mainly hexanes and pentanes [8]. Thus naphtha is able to dissolve more aromatic components than paraffin.

These two techniques require different amounts of solvent for effective operations. Solvent over bitumen ratio (S/B) used in naphthenic froth treatment is 0.65 - 0.7, whereas S/B of paraffinic froth treatment is no less than 2 [6]. During paraffinic froth treatment, partial precipitation of a heavy hydrocarbon constituent (e.g., asphaltenes) occurs [4]. Precipitated asphaltenes in the paraffinic froth treatment vessel can act as flocculants for water droplets and solids. Hence residual water and solids settle with asphaltenes, and this leads to nearly water-free hydrocarbon product after paraffinic froth treatment. Naphthenic froth treatment requires mechanical separation equipment such as inclined plate settlers or centrifuges to reject most of the residual water and solids. It leaves about 1.5 wt% - 2 wt% water and 0.4 wt% - 0.8 wt% solids in the bitumen product [4]. The remaining water in bitumen after naphthenic froth treatment is dispersed as highly

stable water-in-oil emulsions. The majority of the emulsified water droplets are of diameters in the range from 1 μm to 10 μm (mostly as small as 3 μm). The formation of the W/O emulsions is caused by mechanical agitation from pumps, valves or any other transportation related shear [6]. To meet the specification of downstream operations, the total amount of residual water and solids has to be less than 0.5 vol% [9]. In order to achieve this objective, the W/O emulsions formed in naphthenic froth treatment must be destabilized.

1.1.3 Current demulsification process in oil sands processing

Chemical demulsifiers are added during oil sands processing to improve bitumen froth quality and destabilize W/O emulsions [8]. Most of demulsifiers used by oil sands industry are nonionic polymeric molecules, such as acid- or base- catalyzed phenol-formaldehyde polymers, ethoxylated and/or propyloxylated polyamines, di-epoxides, polyols, silicone copolymers, *etc.* [8] [10]. Some ionic demulsifiers are also used to break emulsions formed during oil sands processing, depending on specific processing needs [11].

An important class of nonionic demulsifiers is represented by poly ethylene oxide-poly propylene oxide block (PEO-PPO) copolymers, whose performance has been probed in a number of studies conducted at room temperature [12 - 14].

Currently naphthenic bitumen froth treatment operates at high temperature. For example the Suncor processing operates at 80 °C with S/B about 0.65 [15]. High temperature can improve the demulsification of W/O emulsions through changes to the physical properties of the continuous phase of the emulsions [16 - 17]. The

performance of PEO-PPO copolymers in breaking W/O emulsions at high temperature has not been studied.

On the other hand, the kinetics of demulsification processes is of great interest when seeking optimum industrial operation conditions, such as processing residence time or mechanical mixing intensity. Real-time observation of demulsification processes can reveal the kinetics of demulsification. Recently, a novel instrument allowing real-time in-situ particle sizing, known as Focused Beam Reflectance Measurement (FBRM) has been used in some oil and gas related applications [11] [18 - 21]. FBRM is equipped with a mixing system which allows imitation of industrial processing conditions. It is promising to apply this technique to demulsification kinetics study.

1.2 Objectives and thesis outline

In this work, four PEO-PPO copolymers were evaluated by bottle tests on model W/O emulsions (water-in-toluene diluted bitumen emulsions) at ambient and elevated temperatures. FBRM was used to study destabilization kinetics on model W/O emulsions with the addition of the four PEO-PPO copolymers.

Objectives of this work include:

1. To establish a correlation between the PEO-PPO copolymers properties and their demulsification efficiency.

2. To investigate the effect of temperature and mixing on demulsification.

The present thesis comprises of five chapters.

Chapter 2 provides a literature review and covers fundamentals of demulsification and relevant research on demulsifiers. The impact of temperature and mixing on demulsification is discussed.

Chapter 3 introduces the materials used in this work. Experimental procedures including sample preparation and measurement steps are also included.

Chapter 4 focuses on Results and Discussion.

Chapter 5 summarizes this work. Future work is also included in this chapter.

Chapter 2 Literature Review

2.1 Stabilization mechanisms of W/O emulsions formed in naphthenic froth treatment

After naphthenic froth treatment, 1.5 wt% - 2 wt% of water and 0.4 wt% - 0.8 wt% of solids are remaining in the bitumen [4]. The reason why it is difficult to completely remove residual water is that the residual water and bitumen interact and form extremely stable W/O emulsions during naphthenic froth treatment. To destabilize the W/O emulsions, the factors stabilizing the emulsions need to be probed and removed [6]. Theories related to stabilization of the W/O emulsions are introduced as follows.

2.1.1 Physical properties of bitumen

Compared with conventional oil, bitumen has high viscosity, high density, relatively high metal content and low hydrogen to carbon ratio [4]. The density of Athabasca bitumen ranges from 970 kg/m^3 to 1015 kg/m^3. The fact that bitumen density is so close to the density of water poses challenges for bitumen-water separation. Appropriate solvents are used to dilute bitumen and reduce the oil phase density. Figure 2.1.1-1 shows density changes of bitumen-toluene mixture as a function of toluene weight fraction at room temperature.

Bitumen is described as a very viscous Newtonian fluid, whose viscosity at 20 ºC can be as large as 200,000 mPa•s [22], whereas the viscosity of water at the same temperature is 1 mPa•s only. Bitumen viscosity has a strong dependence on temperature and dilution ratio of solvents. In Figure 2.1.1-2, bitumen viscosity changes as a function of dilution ratio are presented [23].

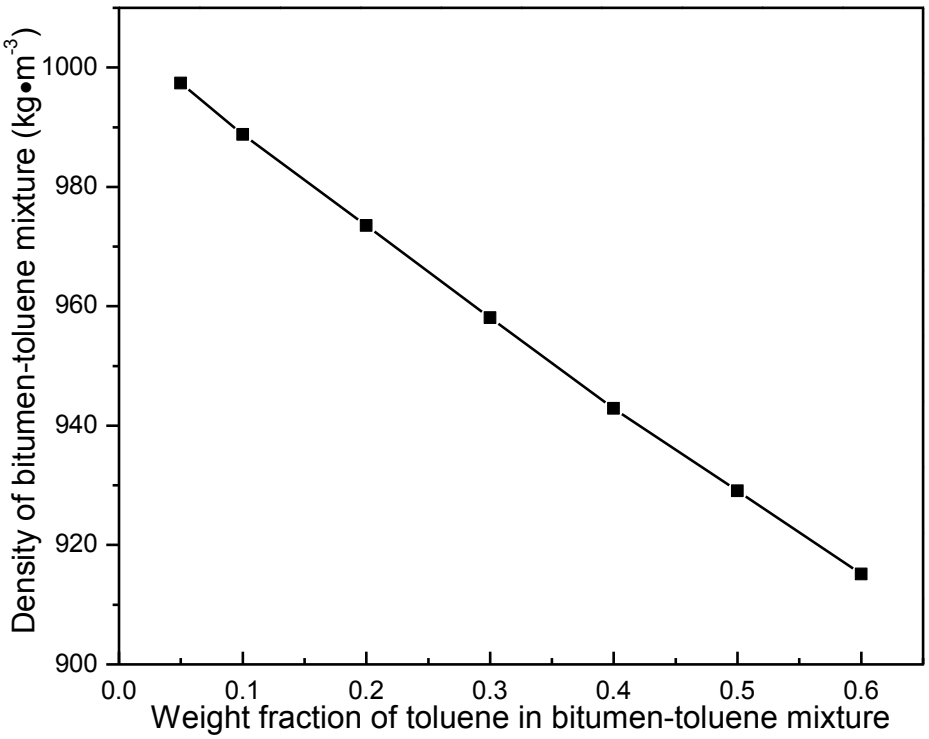

Figure 2.1.1-1 Bitumen density changes with dilution ratio. [24]

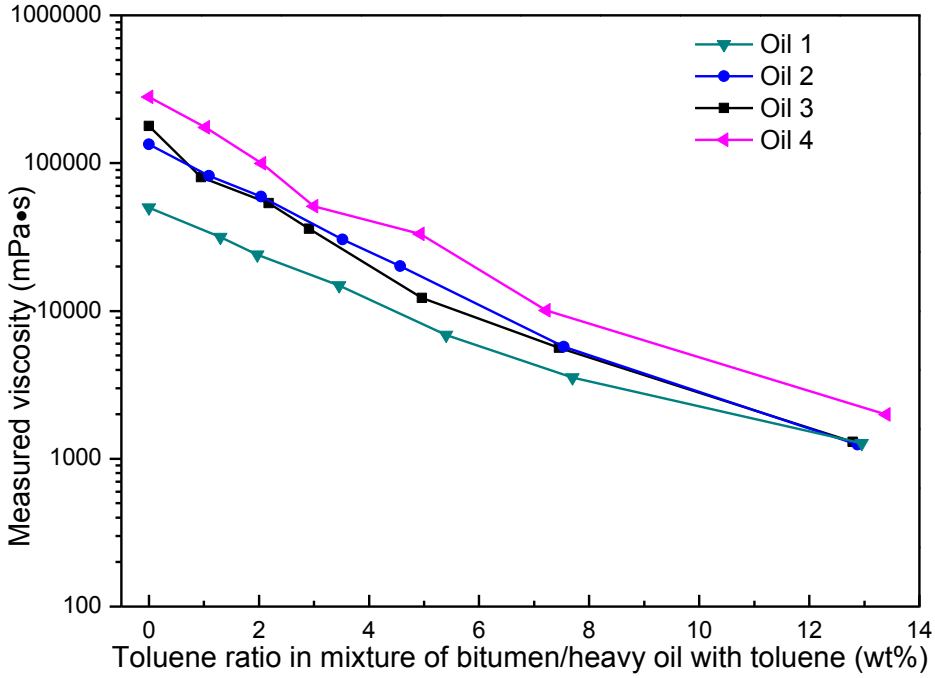

Figure 2.1.1-2 Viscosity changes of Alberta heavy oils as a function of solvent (toluene) content at room temperature. [23]

2.1.2 Chemical characteristics of bitumen

Bitumen consists mainly of carbon and hydrogen. The hydrogen over carbon (H/C) ratio of bitumen is less than 1.55 [25]. Some others elements (heteroatoms) such as sulphur, nitrogen, oxygen, nickel and vanadium are also present at relatively low amounts [26]. Bitumen has extremely complex chemical composition, making it impossible to identify individual compounds of bitumen.

Although to date the composition of bitumen is not fully defined, some compounds and materials present in bitumen are considered to play a major role in the emulsion stability. Such materials are described below [6].

1. Naphthenic acid. Significant quantities of organic compounds in bitumen contain sulfur, oxygen and nitrogen. Some of them are carboxylic acids. Carboxylic acids are the main contributors to the total acid number of crude oil. Carboxylic acids with 10-18 carbon atoms are considered to be naphthenic acids, which are effective surfactants stabilizing W/O emulsions. The sodium salts of the naphthenic acids are also interfacially active [6], which can also act as natural surfactants in bitumen.

2. Clay particles. Clays refer to mineral particles smaller than 2 μm [4]. Clean clay particles are naturally hydrophilic. However, when the particle surface is contaminated by hydrocarbon materials, it can become partially hydrophobic. As a result of surface contamination, clay particles become biwettable to certain degrees [27]. When contaminated clay particles are present in W/O emulsions, the

particles preferentially distribute at the oil-water interface. Figure 2.1.2 illustrates how clay particles having different wettabilities arrange themselves at oil-water interfaces.

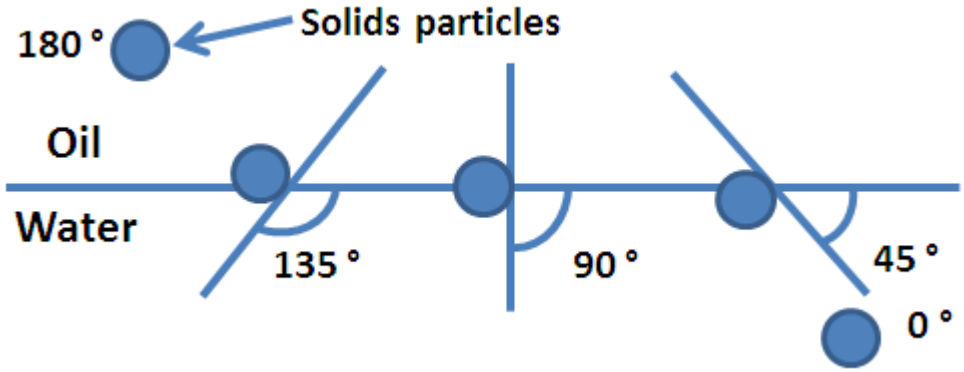

Figure 2.1.2 Clay particles with different wettabilities come into contact with oil-water interfaces. [6]

3. Asphaltenes. Crude oils have complex composition so they cannot be characterized by individual molecular types. Instead, SARA (saturates, aromatics, resins and asphaltenes) group analysis is used to evaluate crude oils constituents. Each group of constituents is separated based on the solubility difference or polarity of molecules in various solvents. Asphaltenes are the heaviest constituent in bitumen based on the fact that they cannot be dissolved in n-pentane or n-heptane (the two solvents commonly used in SARA tests) [28]. Alberta bitumen contains 14 wt% - 20 wt% of asphaltenes [25]. Asphaltenes exist mostly in colloidal forms in bitumen along with strongly polar substances with low molecular weight [29].

Asphaltenes have a strong tendency to aggregate [6]. The consequences of asphaltenes aggregation, such as asphaltenes precipitation during paraffinic froth treatment or unexpected pipeline "plugging" due to asphaltenes precipitates, are of great importance in industrial production of bitumen and heavy oil [30]. Earlier research attributed asphaltenes aggregation and precipitation to the micellization of surfactants in hydrocarbon media [6]. This interpretation was accepted as "colloidal model" and was first introduced by Nellensteyn and refined by Pfeiffer and Saal [6] [31]. A drawback of this model is that the structure of asphaltenes differs from that of surfactants. Since surfactants have polar head and nonpolar tail but asphaltenes do not, it is impossible for asphaltenes to form traditional micelles. It is most likely the poor solubility of asphaltenes in their parent oil that causes the easy phase separation of asphaltenes upon dilution [6] [32 - 33]. Asphaltenes aggregates are believed to build a "gel-like" structure within oil (around dispersed water droplets) and change the rheology of fluid inside the film. Such a change on fluid property hinders water droplet from approaching each other [34].

2.1.3 Stabilization mechanisms of W/O emulsions

The stability of emulsions is essentially dependent on interfacial film properties [6]. When two droplets come into close contact, eventually the liquid film between them becomes so thin that surface forces begin to dominate the interactions between the two droplets [6]. Surface forces include attractive van der Waals forces, repulsive electrostatic force and steric forces [35]. In the case of O/W emulsions, electrostatic repulsion is usually the force playing the most

important role in stabilizing emulsions, whereas in the case of W/O emulsions, steric forces play the major role in hindering water droplets coalescence [36].

For W/O emulsions encountered in naphthenic froth treatment, a layer of materials possibly including natural surfactants, fine bi-wettable particles and asphaltenes are believed to occupy the interface and stabilize the W/O emulsions [6]. In a study using micro pipette technique [37 - 38], water droplets were observed to be covered with rigid films after aging in diluted bitumen solution (0.1 vol% bitumen in 50:50 heptane and toluene solvent). When bitumen was less diluted (10 vol% bitumen in 50:50 heptane and toluene solvent), no rigid film was observed to form during the experiment [38]. Such a film property transition can also be observed when the solvent is naphtha [39] or paraffin [15]. The concentration at which the transition occurs is addressed as "critical concentration" and it varies with the composition of diluents. To investigate the stabilizing components of the W/O emulsions, Wu [40] prepared W/O emulsions with heavy water and solids free bitumen. The author was able to isolate the middle layer between oil and water by centrifugation and collect the adsorbed materials of the oil-water interface. Czarnecki [41] analyzed the interfacial materials obtained from Wu's method by using high-resolution mass spectroscopy. The author found that the average unsaturation degree of the interfacial materials was smaller than 4 (the degree of unsaturation of a benzene ring), indicating that the aromaticity of the interface materials was quite low. This discovery suggests that most of the materials have alkane structures, which is a proof that naphthenic acids are possibly the major components of the interfacial

materials. Czarnecki [42] further summarized the possible stabilizing mechanism of the W/O emulsions by proposing the following model: the abrupt changes on oil-water interfacial properties at critical concentration are likely to be a result of the competition between a subfraction of asphaltenes and natural surfactants. Considering the poor solubility of asphaltenes, its adsorption at interface could be irreversible and the irreversibility of asphaltenic materials' adsorption can exceed the affinity of surfactants to the oil-water interface, especially when bitumen is highly diluted. Additionally, clay particles with certain hydrophobicity also tend to occupy the water-oil interface [6]. The stability of the W/O emulsions is more likely to be a result of the overall interactions among all possible stabilizers [42].

2.2 Demulsifiers

2.2.1 Demulsification mechanisms

To undermine the stability of W/O emulsions in naphthenic froth treatment, film properties of the oil-water interface have to be modified. In chemical demulsification, selected interfacially active materials (demulsifiers) are added to alter interface film properties and promote coalescence and flocculation [43].

Coalescence is the process through which two or more water droplets merge to form a larger water droplet. When two droplets get close to each other, the liquid between them gradually drains. This process is described as fluid film drainage [35]. Eventually the liquid film between two droplets ruptures and a larger droplet forms. To allow the occurrence of the interface film rupture, the film rigidity has to be sufficiently low [6]. The reduction of film rigidity can be achieved by adding demulsifiers [44].

In flocculation, dispersed droplets are bridged together to form flocs. Large flocs can be removed more easily by separation devices than small emulsified water droplets. Droplets within a floc have higher chances to coalesce because they are bound closely. Polymeric demulsifiers can cause flocculation due to their relatively large molecular weight [6].

2.2.2 Demulsifiers used in oil sands processing

Researchers have developed a number of demulsifiers for oil sands processing. Most of demulsifiers used by oil sands industry are nonionic polymeric molecules, such as acid- or base- catalyzed phenol-formaldehyde polymers, ethoxylated and/or propyloxylated polyamines, di-epoxides, polyols, silicone copolymers [8] [10 - 11]. Poly ethylene oxide (PEO) and poly propylene oxide (PPO) copolymer is one common nonionic surfactant used in petroleum industry. For a PEO-PPO copolymer, EO groups act as hydrophilic parts and PO groups act as hydrophobic parts. By adjusting the molar percentage of EO to total moles of EO and PO (EO%), PEO-PPO copolymers with desired amphiphilicity and molecular weight can be produced.

2.2.3 Crucial properties of demulsifiers

To break down the W/O emulsions, demulsifiers must be interfacially active to migrate to oil-water interface and displace the adsorbed layer [6]. Some other important properties need to be considered as well when selecting a demulsifier. For example, to break W/O emulsions, demulsifiers must be able to dissolve well in the oil phase so they can be delivered to the interface through continuous organic phase. Besides, molecular weight and molecular structure of a demulsifier

are also of great importance. Some key factors are summarized in following sections.

Amphiphilicity of demulsifiers

To evaluate the amphiphilicity of a surfactant, an empirical scale of hydrophilic-lipophilic (hydrophobic) balance (HLB) was introduced [45 - 46]. HLB can be evaluated from the ratio of the surfactant solubility in water and oil or calculated using empirical numbers of hydrophilic and lipophilic groups. High HLB values indicate prevailing hydrophilicity, while low HLB values suggest strong lipophilicity. HLB value gives an easy estimation of amphiphilicity of a surfactant.

However, HLB values are only known for a limited number of surfactants. To evaluate the amphiphilicity of surfactants with unknown or complicated structures, relative solubility number (RSN) was defined. The standard definition of RSN is the volume in milliliters of distilled water necessary to produce persistent turbidity when titrating 1 g of surfactant in 30 ml of RSN solvent (benzene-dioxane mixture) [47]. Materials with RSN <13 are nearly insoluble in water. When RSN of a surfactant falls in the range of 13-17, the surfactant is dispersible in water at low concentrations and forms gels at high concentrations, whereas materials with RSN >17 are soluble in water [48]. A modified method developed by Dabros *et al.* [48] uses less toxic toluene-ethylene glycol dimethyl ether (EGDE) as the RSN solvent. By titrating chemicals with known HLB value in the modified RSN solvent, a linear correlation was found between HLB and RSN [48].

Al-Sabagh *et al*. [49] found that alkyldiamine demulsifiers with high HLB values performed better than those with low HLB, indicating that it has a direct relation between HLB value and demulsification efficiency. Schramm *et al.* [50] correlated HLB of demulsifiers and dewatering efficiency in froth treatment using various commercial demulsifiers, including sodium dioctylsulfosuccinate, polyoxyethylene monolaurate, polyoxyethylene sorbitan monopalmita, polyoxylethylene ether and polyoxylethylene amine. The author concluded that demulsifiers with relatively high HLB values (15-20) effectively reduced residual water content without affecting oil recovery. When the system had the highest dewatering efficiency, the oil-water system also had minimum interfacial tension. Fan *et al.* [43] established the correlation between HLB value of polyoxyethylene nonylphenols and their performance by studying their dewatering and interfacial tension changes at different demulsifier concentrations. Pereira *et al.* [51] reported that poor demulsification performance was observed when the demulsifiers used were excessively hydrophilic. It was found that high hydrophilicity (high HLB/RSN values) can cause a significant partitioning of the demulsifier in water phase, resulting in slow demulsifier diffusion. Dabros *et al.* [13] studied a series of diethylenetriamine (DETA)-based PEO-PPO copolymers in destabilization of W/O emulsions involved in oil sands operation. They proved that the RSN number of DETA-based PEO-PPO copolymers is a function of EO%. For PEO-PPO copolymers within the same family, the demulsifier achieved the best dewatering usually has an EO/PO ratio close to 1 [12] [52].

Molecular weight of demulsifiers

Compared with small demulsifier molecules, large demulsifier molecules take relatively long time to diffuse to the oil-water interface. However with long enough residence time or sufficient mixing, demulsifiers with large molecular weight provide superior dewatering performance, as compared with small demulsifiers [53]. In industrial operations, demulsifiers packages used to destabilize W/O emulsions contain both small and large size demulsifiers [53 - 55]. Shetty *et al.* [56] studied demulsification performance of various demulsifiers with molecular weight ranging from 10,000 Dalton to 100,000 Dalton. They found that demulsifiers with low molecular weight performed better than the demulsifiers with high molecular weight. Wu and Dabros reported that demulsifiers with molecular weight in the range of 7,500 Dalton to 15,000 Dalton gave the best performance [52]. Feng *et al.* [57] used ethyl cellulose as demulsifiers to break W/O emulsions. The ethyl cellulose samples with molecular weight between 46,000 Dalton to 182,000 Dalton worked efficiently. The results reported by Pereira *et al.* [51] showed that slow diffusion of large demulsifier molecules slows down demulsification.

Besides HLB value (or RSN) and molecular weight, the molecular structure of a demulsifier also impacts demulsification efficiency. Phukan *et al*. [10] compared the performance of two types of silicone demulsifiers, and found that the silicone demulsifiers with side chains in their structures outperformed the demulsifiers with straight chain structures. Crosslinking is also frequently used to modify the

structure of synthesized polymeric demulsifiers to achieve the highest demulsification efficiency [58].

2.3 Impact of temperature on demulsification

2.3.1 Viscosity reduction of bitumen at elevated temperature

Most of oil sands processing operates at elevated temperature (60 °C - 90 °C) [15] [59]. With an increase in temperature, the bitumen phase would expect a significant viscosity reduction. Figure 2.3.1-1 shows that the viscosity of Athabasca bitumen decreases with increasing temperature. Figure 2.3.1-2 shows that the viscosity of diluted bitumen decreases with an increase in temperature.

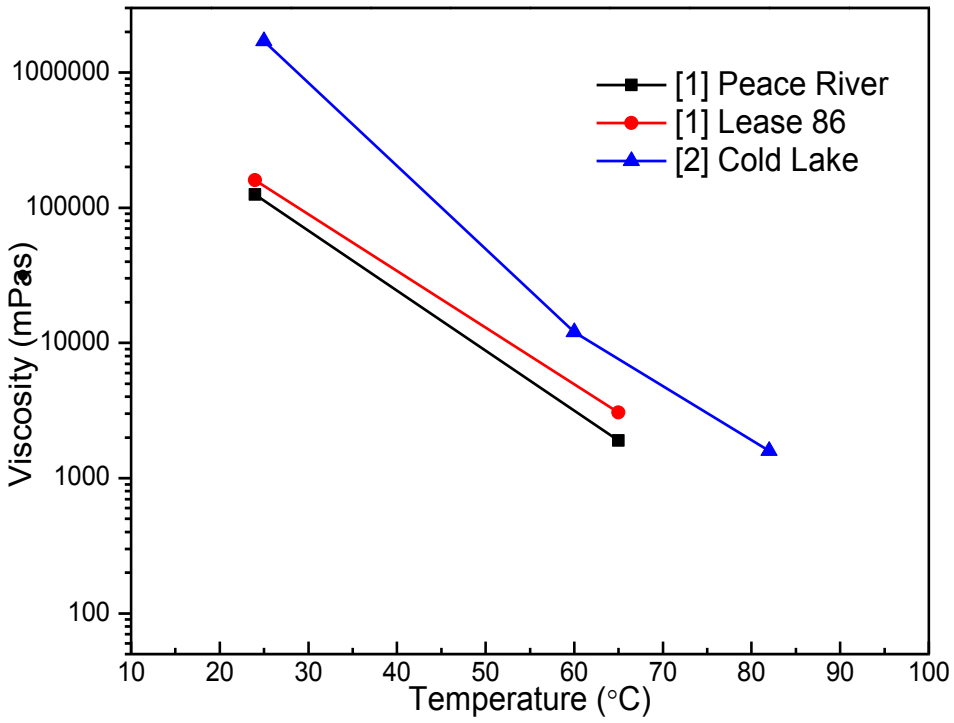

Figure 2.3.1-1 Viscosity of some Alberta bitumen changes as a function of temperature. [60]

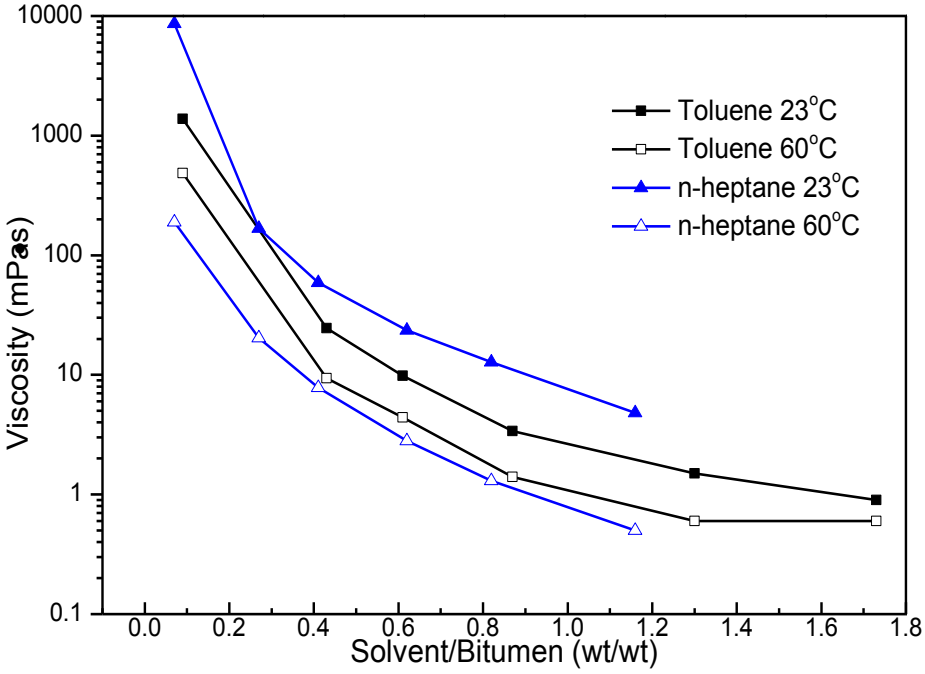

Figure 2.3.1-2 Viscosity of diluted bitumen under various S/B at 23°C and 60°C. [59]

2.3.2 Change of film drainage rate at elevated temperature

Film drainage is described as an important factor influencing demulsification [61]. Theories about film drainage were presented by MacKay and Mason [62 - 63]. According to these theories, film drainage rate V_{Re} is described as follows:

$$V_{Re} = -\frac{dh}{dt} = kh^3 \tag{2-1}$$

$$k = \frac{2\sigma^2}{\mu(\rho_{droplet} - \rho_{bulk})gR^5} \tag{2-2}$$

where h is the film thickness at time t, R is the droplet radius, $\rho_{droplet}$ is the droplet density, ρ_{bulk} is the bulk phase density, μ is the bulk viscosity, σ is the interfacial tension, and g is gravitational constant. Equations 2-1 and 2-2 show that the

reduced viscosity of the continuous phase in an emulsion system can accelerate film drainage.

2.3.3 Sedimentation of water droplets at elevated temperature

The sedimentation of water phase is the ultimate goal of demulsification. The settling process of water droplets is governed partially by Stokes' law [15].

$$U_t = \frac{d_{droplet}^2(\rho_{droplet}-\rho_{bulk})g}{18\mu} \quad (2\text{-}3)$$

where U_t denotes terminal velocity of droplets, $\rho_{droplet}$ and ρ_{bulk} denote droplet density and bulk phase density respectively, μ is bulk phase viscosity and g is the gravitational constant. Stokes' law reveals the relationship between particle settling rate and physical properties of the dispersion. It indicates that low viscosity enhances water droplet settling, which means that increasing temperature can accelerate the sedimentation of water droplets.

Additionally, increased temperature can also enhance Brownian motion and demulsifier's diffusion to enhance demulsification [35].

2.3.4 Temperature impact on PEO-PPO copolymers

The amphiphilicity of PEO-PPO copolymers might be impacted by temperature. Guo *et al.* [64 - 65] studied the conformational changes of PEO-PPO copolymers in the temperature range of 5 °C - 50 °C by FTIR and FT-Raman spectroscopy. They found that increasing the temperature may lower the hydrophilicity of polar EO groups by hindering the formation of hydrogen bonds between EO groups and the aqueous surroundings. Similar findings can be found in numerous studies [66

- 68]. It should be noted that, most of these studies are based on the micellization of water-soluble PEO-PPO copolymers in aqueous phase. However, to demulsify W/O emulsions, the PEO-PPO copolymers should be dissolved in the oil phase, where the impact of temperature may not be as significant as in an aqueous phase.

2.4 Impact of mechanical shear on demulsification

Mechanical mixing can either enhance or hinder demulsification, depending on the specific characteristics of the operations. For example, mechanical shear intensity of a centrifuge is critical for demulsification, because shear-induced coalescence is the main driving force for breaking W/O emulsions [6]. The change of water droplet number caused by shear-induced coalescence can be modeled using the following rule [6]:

$$\frac{dn_{tot}}{dt} = -\frac{16}{3}a^3 G n_{tot}^2 \quad (2\text{-}4)$$

where n_{tot} denotes the number of total droplets at time t, G represents shear rate, a is the distance travelled by droplets before they collide. From Equation 2-4, it is clear that high shear rate can promote coalescence. Fundamental theories and research on shear-induced coalescence can be found in open literature [69 - 71].

However, given the fact that the W/O emulsions formed in oil sands processing are caused by transportation related shear (going through pumps, valves *etc.*), mixing intensity should be controlled at a low level to prevent the formation of more stable emulsions. Additionally, excessive mixing of emulsions also prevents the growth of flocs, which is detrimental for demulsification. For the sake of good

dewatering efficiency, an appropriate mixing rate is needed during demulsification.

2.5 Methods used for demulsifiers evaluation

A variety of methods can be used for demulsifiers evaluation purpose [72]. An easy approach is "bottle test" [14], which is a gravity settling test with the addition of demulsifiers. Usually demulsifiers need to be blended into an emulsion sample before a period of gravity settling. Water removal efficiency was measured to evaluate the demulsifier's performance.

Focused Beam Reflectance Measurement (FBRM) is a particle sizing technique. Thanks to its advanced measurement capacity for in-situ real-time particle size monitoring, FBRM has been applied to study crystallization [73 - 74], hydrate formation [75 - 76], asphaltenes precipitation [18] [77] and in demulsification studies [21].

Boxall *et al.* [19 - 20] [75] [78] applied FBRM technique to study crude oil emulsions. They systematically probed the accuracy of FBRM technique by comparing its results with other particle sizing instruments, including a particle video microscopy (PVM) and an optical microscope. They found that FBRM always gave consistent measurement results for materials with the same texture. Nguyen *et al.* [11] investigated water droplet size changes during demulsification using a combination of FBRM and PVM. They reported that coalesced water droplets were observed immediately after the addition of demulsifier solutions during demulsification. Coalescence of water droplets was finished in a short

period of time (3 min) after the addition of demulsifier solution. Less *et al*. [21] studied oil-water separation inside an electrical dehydrator vessel using FBRM with the assistance of demulsifiers. The authors successfully correlated water droplet size increase with operational factors (concentration of added demulsifiers and electric field intensity).

2.6 Summary of literature review

Previous work on the W/O emulsions formed in naphthenic froth treatment reveals that the layer of interfacially adsorbed materials is responsible for the stability of the W/O emulsions. Demulsifiers with appropriate properties can alter the oil-water interfacial properties and lower the emulsions stability. Increasing temperature can assist the demulsification of the W/O emulsions mainly by reducing bitumen viscosity and accelerating the settling of water droplets. Mixing involved in demulsification needs to be well controlled to ensure demulsification efficiency. Demulsification study using PEO-PPO copolymers at ambient temperature established the correlation between the amphiphilicity of the copolymers and their demulsification performance. However, given the possibility of the hydrophilicity loss of PEO-PPO copolymers at elevated temperature due to conformational changes, it is worthy to study the high temperature demulsification performance of PEO-PPO copolymers. It is also meaningful to investigate the kinetics of demulsification under mixing via real-time observation, which can be achieved with the application of FBRM. Conventional demulsifier evaluation methods including bottle test, interfacial tension measurement and

viscosity measurement will be collaborated with FBRM to accomplish the research objectives.

Chapter 3 Materials and Methods

3.1 Materials

ACS Toluene (99.9% pure) was purchased from Fisher Scientific and used as received. Deionized water (DI water) was used throughout the study.

Vacuum distillation feed bitumen used for W/O emulsions preparation was provided by Syncrude Canada Ltd. The bitumen was diluted with toluene to obtain a solvent to bitumen ratio (S/B) of ~0.66 (i.e., the solution contained 60 wt% bitumen and 40 wt% toluene). The bitumen and toluene mixture was placed in a mechanical shaker and kept shaking for more than 4 h to allow for complete mixing. Solids were removed from the diluted bitumen by centrifuging the oil at 14,000 g force for 30 min. The diluted bitumen solution prepared according to this protocol was used throughout the current study.

Four PEO-PPO copolymers were provided by an industrial supplier. Their properties are listed in Table 3.1. Stock solutions of 1 wt% demulsifier in toluene were freshly prepared and diluted to desired concentration before each experiment.

Table 3.1 Properties of the four PEO-PPO copolymers.

Chemical	A	B	C	D
EO%	35	20	35	5
Molecular Weight (Dalton)	12311	10003	6145	8423
Arm Number	5	5	3	5
RSN	18.07	10.59	16.92	7.92

3.2 Preparation of W/O emulsions

W/O emulsions used in FBRM tests were prepared with 1.58 g of DI water and 30 g of diluted bitumen. The mixture was homogenized using a PowerGen1000 homogenizer (Fisher Scientific, United States) at 30,000 rpm for 3 min. The resulting emulsion contained 5 wt% of water. W/O emulsions used for bottle tests were prepared using 0.39 g DI water and 7.4 g diluted bitumen and homogenized as described above.

Water droplets in the emulsions prepared as described above were smaller than 5 μm in diameter, as determined with an optical microscope. A typical micrograph of the emulsion water droplets is shown in Figure 3.2.

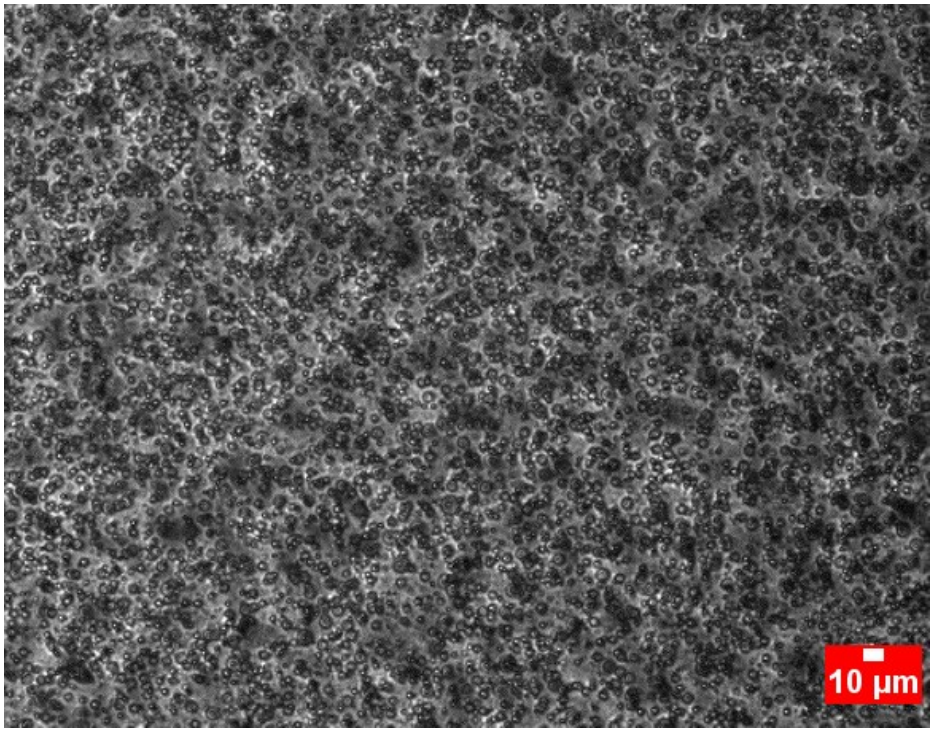

Figure 3.2 Dispersed water droplets of the W/O emulsion used in this work.

3.3 Interfacial tension measurement

DI water was used as aqueous phase to interact with diluted bitumen phase. Interfacial tension measurements were completed with the Du Nouy ring method using a Kruss Processor Tensiometer K12 (Kruss, Germany), equipped with a Pt-Ir ring. Measurements were taken at room temperature (22.2 ^{o}C – 23.5 ºC) and 60 °C.

For each room temperature test, a desired amount of demulsifier solution was pre-mixed with diluted bitumen at 220 rpm for 3 min and carefully poured on the water phase in the tensiometer cup. The system was allowed to equilibrate for 1 h prior to each measurement.

For high temperature measurements, the mixture of diluted bitumen and demulsifier solution was heated to 60 °C and subsequently poured on the top of the aqueous phase. An external circulating water bath was used to maintain the sample temperature constant at 60 °C. Similar to the room temperature case, the system was allowed to equilibrate for 1 h before each measurement.

Dynamic interfacial tension of toluene-water interface as a function of PEO-PPO copolymers concentration was measured by Attention Optical Tensiometer (Biolin Scientific, Sweden) to investigate the adsorption kinetics of the four copolymers at toluene-water interface at room temperature. Pendant drop method was used to measure the dynamic interfacial tension. Toluene solutions of the four demulsifiers were used as the oil phase. To initiate a measurement, a DI water droplet was created on the tip of a syringe in the toluene solution of the

demulsifiers. Each measurement was controlled to be sufficiently long to make sure the system arrived equilibrium state.

3.4 FBRM study of demulsification kinetics

Focused Beam Reflectance Measurement (FBRM) was utilized to probe the kinetics of demulsification using the four PEO-PPO copolymers described in section 3.1. FBRM is a particle sizing instrument which is designed to measuring the sizes of particles in real time. It is able to measure in-situ particles and droplets of concentrated suspensions or emulsions without extraction or dilution. The details regarding this technique are introduced in the following sections.

3.4.1 FBRM technique

A description of FBRM probe and its accessories

FBRM can measure particles between 0.5 μm – 2.5 mm [79]. The working principle of FBRM is based on backscattering of laser beam. A FBRM probe needs to be inserted into suspensions or emulsions to monitor the size change of particles or droplets. Figure 3.4.1-1 shows a schematic of a FBRM probe. Figure 3.4.1-2 shows the components of FBRM measurement system.

A FBRM probe consists of a sapphire window and two optics modules. During a measurement, the laser is focused in a focal plane outside the window surface after passing through the optics module. The focused beam rotates at a speed of 2 m/s - 8 m/s around the probe window [79]. When a particle passes the focal plane, the focused beam interacts across one edge of the particle and backscatters the laser light until the beam reaches the opposite edge of it. The backscattered light

is collected by the FBRM optics and converted into electronic signals that are sent back to a terminal control computer. A solid-state laser light source is used to produce continuous monochromatic light (infrared laser, Class 1) for measurements [79]. Terminal control software installed in the computer is used to display the real-time measurement results.

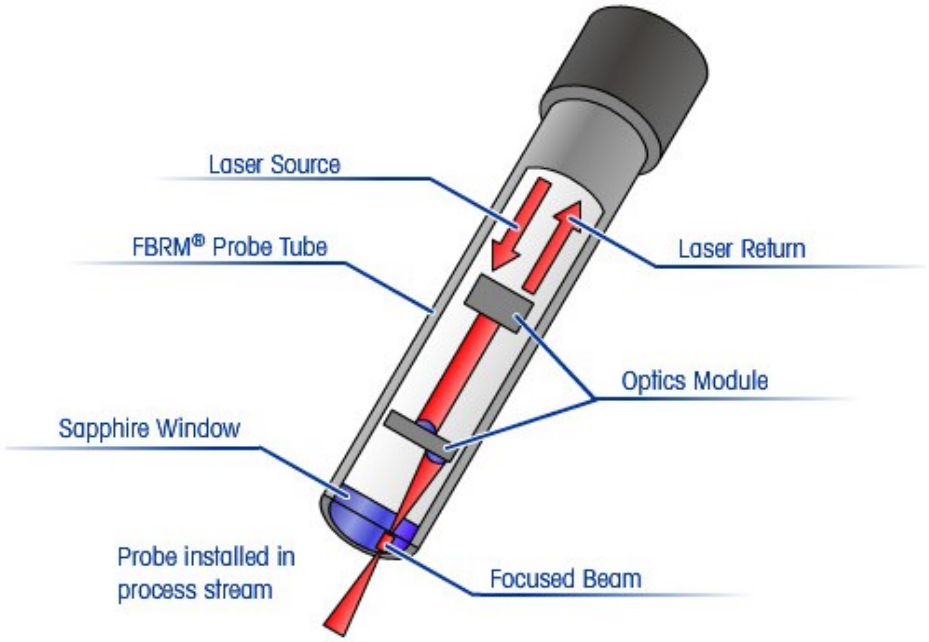

Figure 3.4.1-1 FBRM probe. [79]

FBRM requires continuous mixing of the suspension during measurements to collect representative data. Particle movement due to mixing has a negligible influence on measurements because the revolving speed of the laser beam is much faster than particle movement. Selecting an appropriate mixing rate is crucial for a FBRM measurement. Excessive mixing can disrupt aggregation or crystallization and result in decrease of particle sizes, thus leading to biased results. Over-mixing can also generate gas bubbles that interfere with measurements. Conversely,

insufficient mixing possibly causes sedimentation of large dispersed droplets leading to inaccurate measurement results. Figure 3.4.1-3 gives a schematic of Fixed Beaker Stand (FBS), which holds the standard mixer of FBRM.

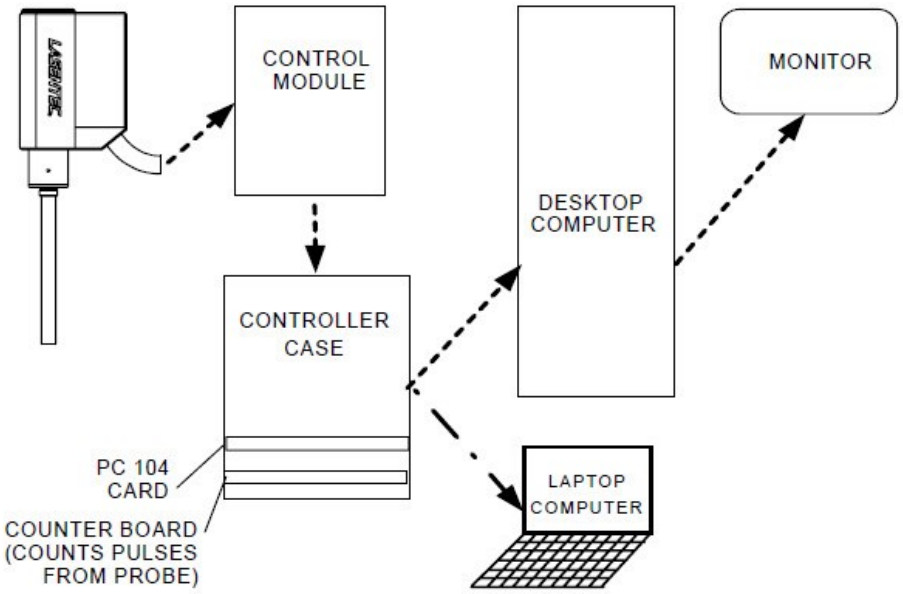

Figure 3.4.1-2 A schematic of FBRM working station. [79]

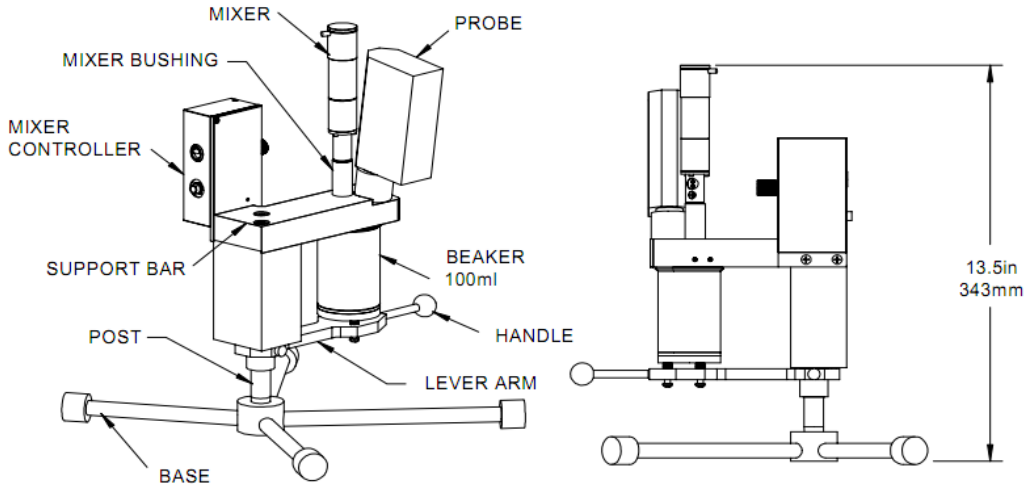

Figure 3.4.1-3 Fixed beaker stand. [79]

The mixer is equipped with a pitch blade turbine impeller. The angle between FBRM probe and the mixer impeller is about 30°. This system ensures that the FBRM probe and the impeller stay at the same position during each measurement.

Data collection of FBRM

During FBRM measurements, when the laser beam intersects a single particle from its one edge to the opposite edge, the corresponding reflection time of backscattered laser is detected. The reflection time is recorded and multiplied by the scanning speed of the laser beam to obtain the chord length. The chord length represents the size of the particles present in a suspension. Since the radius of the laser's revolution is much larger than the particle size range, the chord length can be approximated to be the length of a straight line between the two points where the beam intersects with the particle's boundary [79]. Figure 3.4.1-4 shows how chord lengths are measured.

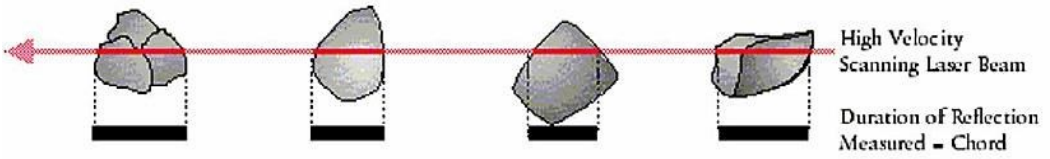

Figure 3.4.1-4 Chord length measurement by laser beam scanning. [79]

The quantity of particles measured by FBRM can also be recorded. The counts per second of a size group represent the number of particles whose sizes fall in the specific size bin detected by FBRM. For example, if 100 particles having a diameter <10 μm in the suspension are scanned by the rotating laser beam in one second, the counts per second of <10 μm particle group is 100. The mean size of

the particles in the suspension can be calculated from the chord length distribution and counts per second. FBRM software estimates two types of mean sizes: non-weighted median and square weighted median, which are approximated to number mean and volumetric mean (Sauter mean), respectively. The mathematical expressions of non-weighted median and square weighted median are as follows [20]:

$$L_{mean}(non-\ weighted) = \frac{\sum_{1\le i\le M} f(i) l_i}{\sum_{1\le i\le M} f(i)} \qquad (3\text{-}1)$$

$$L_{mean}(square\ weighted) = \frac{\sum_{1\le i\le M} f(i) l_i^3}{\sum_{1\le i\le M} f(i) l_i^2} \qquad (3\text{-}2)$$

where $f(i)$ denotes the probability of particles whose chord length is l_i. From these two equations, it can be seen that volumetric mean size emphasizes the influence of large particles in the system.

3.4.2 Demulsification tests using FBRM

Selection of an appropriate mixing speed for demulsification

31.58 g W/O emulsion (5wt% water) was prepared in a 100-milliliter glass beaker. Before introducing the demulsifier solution into the emulsion sample, mixing stability of the emulsion was tested at different mixing speeds in order to assess that, prior to demulsifier addition, the droplet size remained constant at the mixing conditions. The emulsion sample was stirred at room temperature at different mixing speeds, namely 100 rpm, 220 rpm, 320 rpm and 400 rpm. The data show that the mean droplet sizes were almost constant with all stirring speeds.

The impact of mixing on demulsification was tested for the demulsifiers described in section 3.1 using speeds of 100 rpm, 220 rpm, 320 rpm and 400 rpm. These tests were allowed to define the mixing speed at which the droplet size increase was the greatest. The identified speed was subsequently used in the tests for demulsification kinetics study.

Demulsification kinetics of the four PEO-PPO copolymers

The same amount of W/O emulsions (31.58 g) was used in each measurement of FBRM demulsification tests. Blank tests were first completed at room temperature and 60 ^{o}C as references. For the blank test of high temperature, an external circulating water bath was used to keep the emulsion temperature constant at 60 °C.

For each room temperature FBRM demulsification test, the emulsion sample was stirred for 5 min without adding any demulsifier to determine the initial water droplet size distribution. Following the 5 min equilibration time, a desired amount of demulsifier solution was added and the water droplet size was monitored over a 30 min time period.

For each high temperature FBRM demulsification test, a water bath was used to keep the emulsion temperature constant at 60 °C. The sample was covered by aluminum foil to limit sample evaporation. Once the temperature of the emulsion reached 60 °C, the water droplet size distribution was measured for 5 min, after which the demulsifier solution was injected in the system and the droplet size was measured for an additional 30 min.

All FBRM demulsification tests were repeated at least twice. Table 3.4.2 lists all experimental conditions used in FBRM demulsification tests. Remaining water content of the emulsion samples after FBRM demulsification was measured by a Cou-Lo 2000 Karl Fischer titrator. At least three measurements were performed for each sample and the averaged result was taken as the remaining water content of the sample.

Table 3.4.2 Experimental conditions used in FBRM demulsification tests.

Dosage / Temperature	Demulsifier A (ppm[a])			Demulsifier B (ppm)			Demulsifier C (ppm)			Demulsifier D (ppm)		
Room temperature	10	50	100	10	50	100	10	50	100	10	50	100
60 ºC	10	50	100	10	50	100	10	50	100	10	50	100

ppm[a] (mg/kg): 1 milligram of demulsifier per kilogram of the oil phase (diluted bitumen)

3.5 Evaluation of the four PEO-PPO demulsifiers by bottle test

Bottle tests were conducted to evaluate the dewatering performance of the four PEO-PPO copolymers described in section 3.1.

For room temperature bottle tests, a desired concentration of demulsifier solution was injected into 7.8 g of the W/O emulsion to initiate demulsification immediately after the emulsion preparation. A Fisher Labdisc stirrer was used to blend demulsifier into the emulsion phase at approximately 300 rpm for 0.5 - 5 minute(s). Emulsion samples were then transferred to 11-millimeter Pyrex glass

tubes (16×100 mm) to settle for 1 h. After gravity settling, the water content of the emulsion sample was measured at 2 cm below the top surface.

For high temperature tests, emulsion samples were heated to desired temperature. Demulsifier solution was introduced to the W/O emulsions and blended for 0.5 - 5 minute(s). Emulsion samples were transferred to 11-milliliter Pyrex glass tubes and placed in a water bath at 60 °C for 1 h. The remaining water content was measured following the same procedure as used for room temperature measurements.

The experimental conditions of bottle tests are summarized in Table 3.5-1 and Table 3.5-2.

Table 3.5-1 Experimental conditions used in bottle tests.

Demulsifier	A			B		
Dosage (ppm[a])	10	50	100	10	50	100
Demulsifier	C			D		
Dosage (ppm)	10	50	100	10	50	100

ppm[a] (mg/kg): 1 milligram of demulsifier per kilogram of oil phase (diluted bitumen)

Table 3.5-2 Blending time used in bottle tests.

Blending time	30 s	1 min	2 min	3 min	4 min	5 min

Control tests without demulsifier addition were performed at ambient temperature and 60 °C. For the control tests, samples were blended for either 0.5 minute or 5 minute (the minimum mixing and the maximum mixing time) before 1 h settling.

3.6 Effect of temperature on viscosity of diluted bitumen

Viscosity of the diluted bitumen was measured by an AR-G2 rheometer (TA Instruments, USA) at 25 ^{o}C and 60 ^{o}C. Sample temperature was regulated by a Peltier plate temperature control system. The internal resolution of the Peltier plate is within ±0.01 ºC. The AR-G2 rheometer was equipped with a water bath to assist the Peltier plate to achieve temperature adjustment. Since cone plate geometry can be used to measure samples with a wide range of viscosity, a cone-plate geometry was utilized to measure the sample viscosity at room temperature. A concentric cylinder geometry that is suitable for low viscosity measurement was combined with a metal cap to measure the viscosity of the sample at 60 ^{o}C.

For room temperature measurements, initially about 5 g of the diluted bitumen was loaded on the top of the Peltier plate. The cone plate then started to apply shear force on the sample. As a result of shear, overloaded bitumen would be forced beyond the rim of the cone plate. After removing extra sample from the Peltier plate, the cone plate sheared the remaining sample for a 5 min equilibrium period before measuring the sample viscosity, mainly for the purpose of structural effects elimination.

For high temperature measurements, 8 g of diluted bitumen was transferred into the concentric cylinder geometry. The standard rotor of the concentric cylinder was lowered below the top of the diluted bitumen sample and started shearing. The cylinder was covered by the metal cap to limit evaporation. After the sample was

heated to 60 ^{o}C, a 5-min of equilibrium period was set before measuring the sample viscosity to eliminate structural effects and temperature gradient within the sample.

Chapter 4 Results and Discussion

In the present chapter, interfacial tension measurement results, data of the FBRM demulsification tests, remaining water content obtained from the bottle tests and viscosity measurement results are shown together with related discussion.

4.1 Interfacial tension

4.1.1 Ability of the demulsifiers in lowering interfacial tension

To probe the ability of the demulsifier to adsorb at the diluted bitumen-water interface, interfacial tension was measured at different demulsifier dosages. Figure 4.1.1 shows the interfacial tension of the system at room temperature as a function of mass concentration and molar concentration of the demulsifiers.

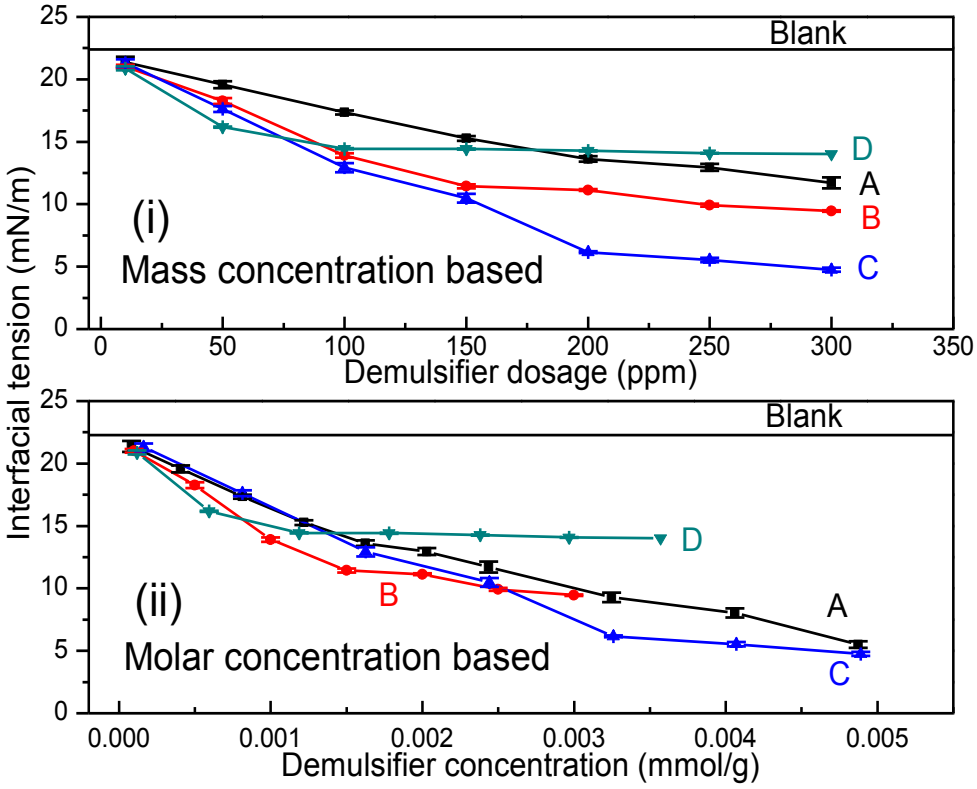

Figure 4.1.1 Interfacial tension between diluted bitumen and DI water in the presence/absence of the four demulsifiers at room temperature.

The data reveal that all the four PEO-PPO demulsifiers were able to further lower the interfacial tension of the diluted bitumen-water interface, indicating the ability of the demulsifiers to compete for interface. The trend in Figure 4.1.1 reveals that, for a given mass addition, demulsifier C was the most effective in lowering interfacial tension, whereas demulsifier D was the least effective. The curve of demulsifier B was between the curves of demulsifier D and demulsifier C, possibly suggesting that the ability of demulsifier B to compete for the interface was greater than that of demulsifier D and less than that of demulsifier C. It is noted that at the same molar concentration, demulsifier A and demulsifier C reduced interfacial tension to a similar level, whereas demulsifier A was not as effective as demulsifier C at the same dosage (*cf.* Figure 4.1.1 (i)).

To understand the ability of the four PEO-PPO copolymers to lower diluted bitumen-water interfacial tension, the demulsifier structure needs to be considered. Among the four demulsifiers, demulsifier D contains the most hydrophobic PO groups as compared with the other three demulsifiers. The high PO content of demulsifier D caused the demulsifier molecules to partition preferentially in the oil phase rather than adsorb at the diluted bitumen-water interface [49] [80].

In contrast to demulsifier D, demulsifier A and demulsifier C both have very high EO content (EO%=35%), and demulsifier B contains less EO (EO%=20%) than demulsifier A and demulsifier C. The strong ability of demulsifiers A and C in

reducing interfacial tension proves that when demulsifiers contain more hydrophilic components in their structures, their ability to reduce interfacial tension is improved. The results of interfacial tension reduction indicate that demulsifier A, demulsifier C and demulsifier B have relatively strong affinity for diluted bitumen-water interface.

If added demulsifier molecules have strong affinity to oil-water interface, they can compete for the interface and displace the pre-adsorbed materials at the interface to reduce interfacial tension of the system [6]. Feng *et al.* [53] once reported the affinity of ethyl cellulose (EC) molecules to oil-water interface using interfacial tension measurement. The dewatering efficiency of EC was found to be correlated to the affinity of EC to the oil-water interface. Atta *et al.* [81] studied the dewatering performance of some PEO-PPO copolymers. The authors found that successful dewatering occurred when the interfacial tension of the system was effectively reduced by the addition of PEO-PPO copolymers. However, although the demulsifiers can effectively lower interfacial tension, they might not necessarily be effective in breaking the emulsions [12] [82].

4.1.2 Effect of temperature on the ability of demulsifiers to lower interfacial tension

Figure 4.1.2 shows the interfacial tension of the diluted bitumen-water interface at room temperature and 60 °C in the presence of various amounts of demulsifiers. The data showed that the interfacial tension of the diluted bitumen-water interface in the presence of demulsifiers A, B and C were slightly lower at 60 °C than at room temperature. In contrast, the interfacial tension measured upon addition of

demulsifier D was lower at room temperature than at 60 °C. This finding indicates that demulsifier D may partially lose its affinity to interface at 60 °C, which might yield less efficient demulsification.

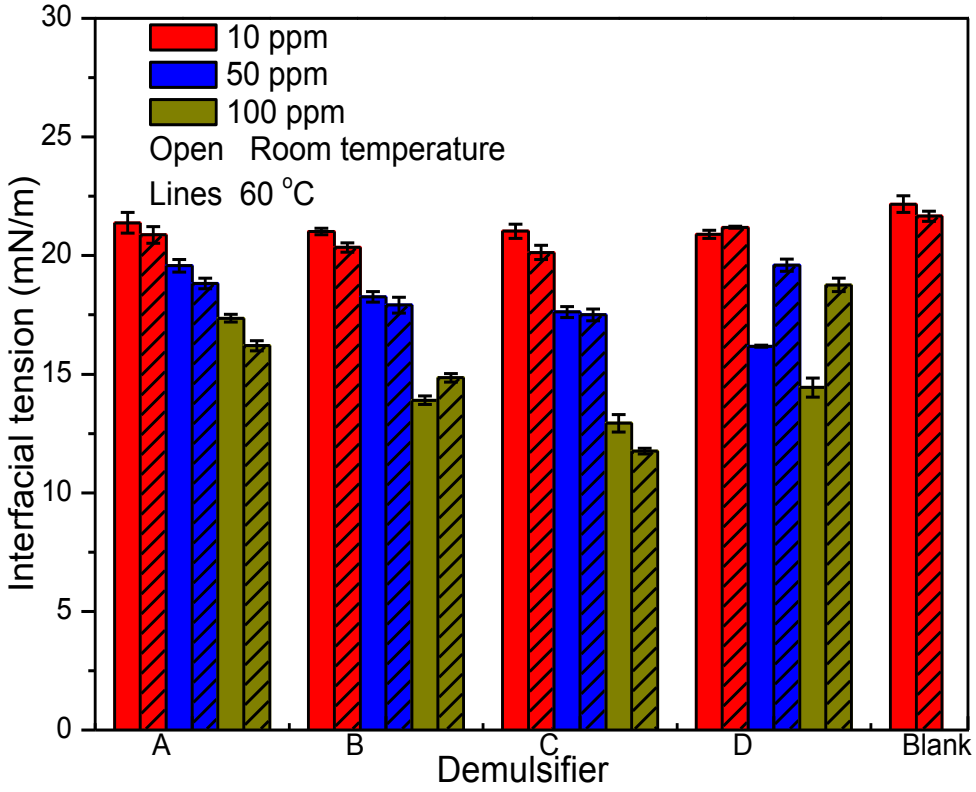

Figure 4.1.2 Effect of temperature on interfacial tension.

The hydrophilicity loss of demulsifier D may be related to its structural characteristics. Demulsifier D has the lowest EO% among the four PEO-PPO copolymers. Some previous studies [64 - 65] reported that high temperature may lower the hydrophilicity of PEO-PPO copolymers by causing changes in the hydrogen bonds between EO groups and water molecules of the aqueous phase. Therefore the ability of a PEO-PPO copolymer to lower interfacial tension can be hindered at increased temperature, as was observed for demulsifier D in this

study. The other three demulsifiers have high EO% and are thus highly hydrophilic. Such considerations may explain why demulsifier D was affected the most by the temperature increase.

4.1.3 Dynamic interfacial tension measurement

Dynamic interfacial tension measurement allows us to evaluate the adsorption kinetics of the demulsifiers at oil-water interface [83]. To avoid the interference from film displacement occurring at the diluted bitumen-water interface when observing the adsorption of the demulsifier molecules, the interface of toluene-water system was selected to study the affinity of the four demulsifiers to oil-water interface. To compare the ability of the four demulsifiers competing for the interface, the measurements were completed at fixed dosages, namely 1 ppm, 2 ppm and 5 ppm. Figure 4.1.3 shows the interfacial tension reduction of the toluene-water interface as a function of time after water droplets were created in the demulsifiers' toluene solutions.

The interfacial tension of pure toluene-water interface at room temperature is 36 mN/m [84]. In Figure 4.1.3, the initial interfacial tension of the system at each condition was around 35 mN/m. After the water droplet was created in the toluene phase, the interfacial tension of the system started to decrease as a result of demulsifier adsorption at the interface. It shows that the interfacial tension reduction was dependent on demulsifier concentration. It took different periods of time for the system to reach equilibrium in the presence of the four demulsifiers. Differing from the static interfacial tension measurement, demulsifiers A and C had similar performance under the same mass concentration. These two reduced

the interfacial tension of the system most effectively at all dosages. This is understandable considering that demulsifiers A and C have the highest EO% (35%). The systems containing demulsifier D reached equilibrium state over the shortest time. However, the final interfacial tensions of the systems containing demulsifier D were the highest at the tested conditions, owing to the fact that demulsifier D is the most hydrophobic among the four demulsifiers. Demulsifier B had intermediate performance regarding interfacial tension reduction, which can be explained by its moderate hydrophilicity.

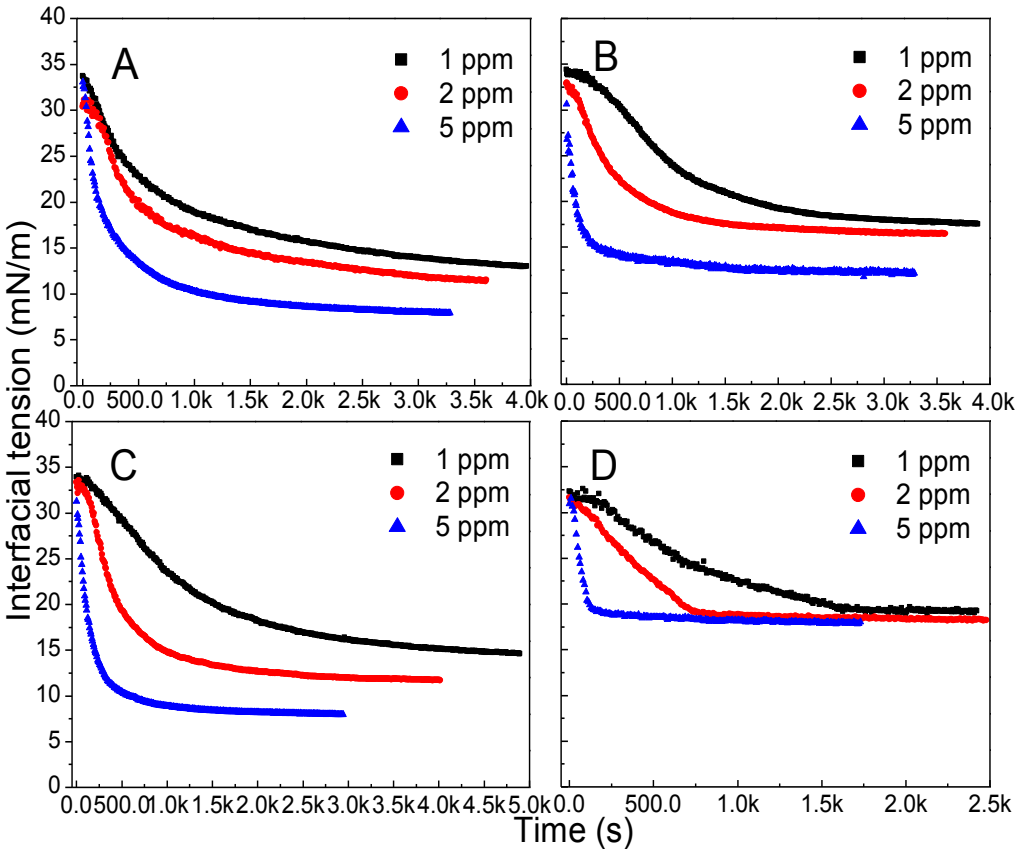

Figure 4.1.3 Dynamic interfacial tension changes of toluene-water interface in the presence of various concentrations of the four demulsifiers.

4.2 FBRM tests

4.2.1 Effect of mixing rate on demulsification

Figure 4.2.1-1 shows the mean sizes and counts changes of emulsion water droplets at different stirring speeds.

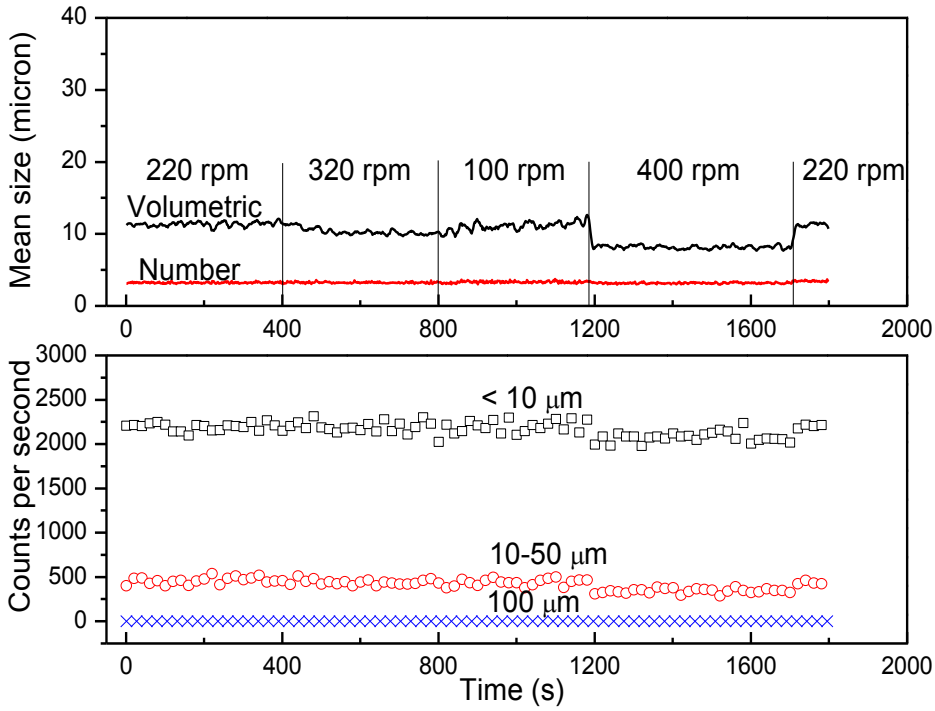

Figure 4.2.1-1 Effect of mixing rate on mean size and counts of an emulsion sample at room temperature without demulsifier addition.

Figure 4.2.1-1 shows that the number mean of the water droplets hardly changed with stirring speed. The volumetric mean was reduced by 2 μm at 400 rpm than at other lower stirring speeds, possibly due to reduced attachment between droplets under strong mixing. Counts of different size bins were constant during the test.

Based on the base lines results given in Figure 4.2.1-1, demulsification by demulsifier B at various mixing speeds was selected as an example to illustrate

the effect of mixing on demulsification. Figure 4.2.1-2 shows the mean size change of water droplets in demulsification with 50 ppm of demulsifier B at room temperature.

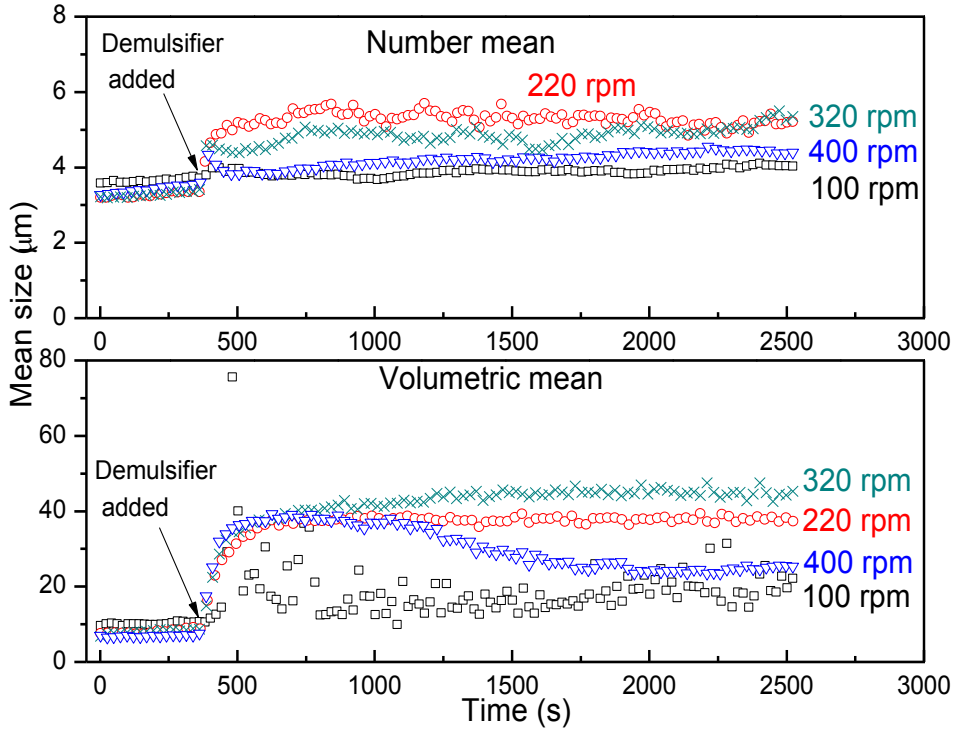

Figure 4.2.1-2 Impact of mixing speed on demulsification using 50 ppm of demulsifier B at room temperature.

The changes of volumetric mean show that 100 rpm was not sufficient to promote effective coalescence. At 400 rpm, the volumetric mean increased from 8 μm to 38 μm upon the addition of demulsifier B, but it begun to decrease after 1200 s, indicating that coalesced water droplets or flocs were disrupted by strong mixing. Mixing at 220 rpm and 320 rpm produced relatively consistent volumetric mean size growth. The number mean size changes show that 220 rpm increased the

water droplets size smoothly and stably. Therefore 220 rpm was used in the following FBRM tests to study the effects of other factors on demulsification.

4.2.2 Demulsification kinetics study

Blank tests at room temperature and 60 °C

Figure 4.2.2-1 shows the mean size and counts of the emulsion water droplets of room temperature blank test without the addition of demulsifiers.

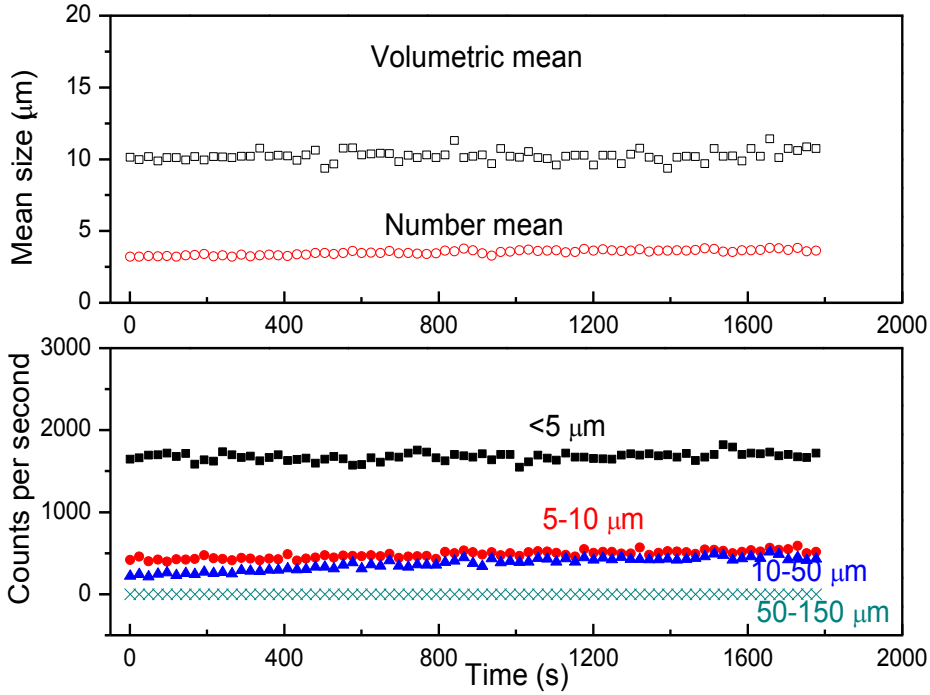

Figure 4.2.2-1 Mean sizes and counts of the emulsion water droplets in room temperature blank test.

Figure 4.2.2-1 shows that the size of water droplets in the system underwent negligible changes during the tested period. The volumetric mean size and the number mean size of the emulsion water droplets were 10 μm and 3 μm, respectively. The counts of water droplets having a diameter <5 μm and between

5 μm - 10 μm were approximately 1700 and 500, respectively. The counts of droplets having a diameter between 10 μm - 50 μm were around 400. Water droplets having a diameter >50 μm were not detected. Results of the blank test ensured that the emulsion was sufficiently stable under the mixing conditions.

Figure 4.2.2-2 shows mean size and counts of water droplets of blank test at 60 °C.

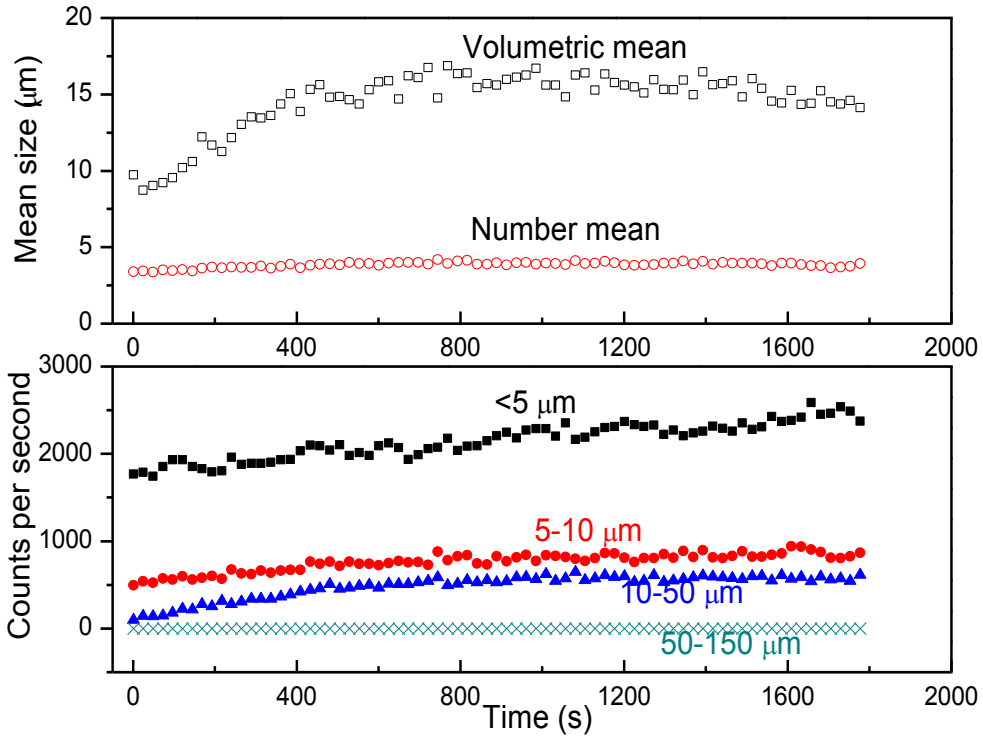

Figure 4.2.2-2 Mean size and counts of emulsion water droplets at 60 °C.

Droplet sizes measured in 60 °C blank tests are shown in Figure 4.2.2-2. The sample temperature was increased from room temperature to 60 °C in the first 400 s. The data showed that the temperature increase had negligible impact on the number mean (around 3 μm) of the system. The volumetric mean increased from

10 μm to 15 μm in the first 400 s as a result of heating. The counts of water droplets having a diameter <5 μm increased from 1800 to above 2500. The counts of water droplets between 5 μm - 10 μm increased gradually from 500 to 700 during the test. The counts of droplets having a diameter between 10 μm – 50 μm increased from around 50 to 500. It is worth noting that no counts decrease was observed for small water droplets (<5 μm) whereas the counts of larger water droplets (5 – 50 μm) increased. The extra droplets occurred in the system due to heating indicated that some very small water droplets were generated by homogenizing during the emulsion preparation. Those water droplets were so small that FBRM was not able to detect them (FBRM measurement limit: 0.5 μm - 2.5 mm). The increase in the counts of both small and medium size water droplets, together with the increase in the volumetric mean of the system proved that heating can induce coalescence of the emulsion water droplets to a certain extent. However, the coalescence induced by heating was limited since the volumetric mean of the system equilibrated again after the sample temperature reaching to 60 °C.

Selection of a representative mean size to interpret the demulsification kinetics

Demulsification tests of demulsifier B at room temperature were selected as an example to illustrate the investigation of demulsification kinetics (Figure 4.2.2-3). Figure 4.2.2-3 shows that, following the addition of demulsifier B, the size of the water droplets begun to grow after 300 s. The volumetric mean and number mean of the water droplets plateaued after 180 s, reaching 38 μm and 7 μm,

respectively. The increase in droplet size due to either flocculation or coalescence of the smallest water droplets in the system resulted in a decrease in the counts of the water droplets having diameter <5 μm. The volumetric mean size had a significant increase compared with the limited change of the number mean size upon the addition of demulsifier solution.

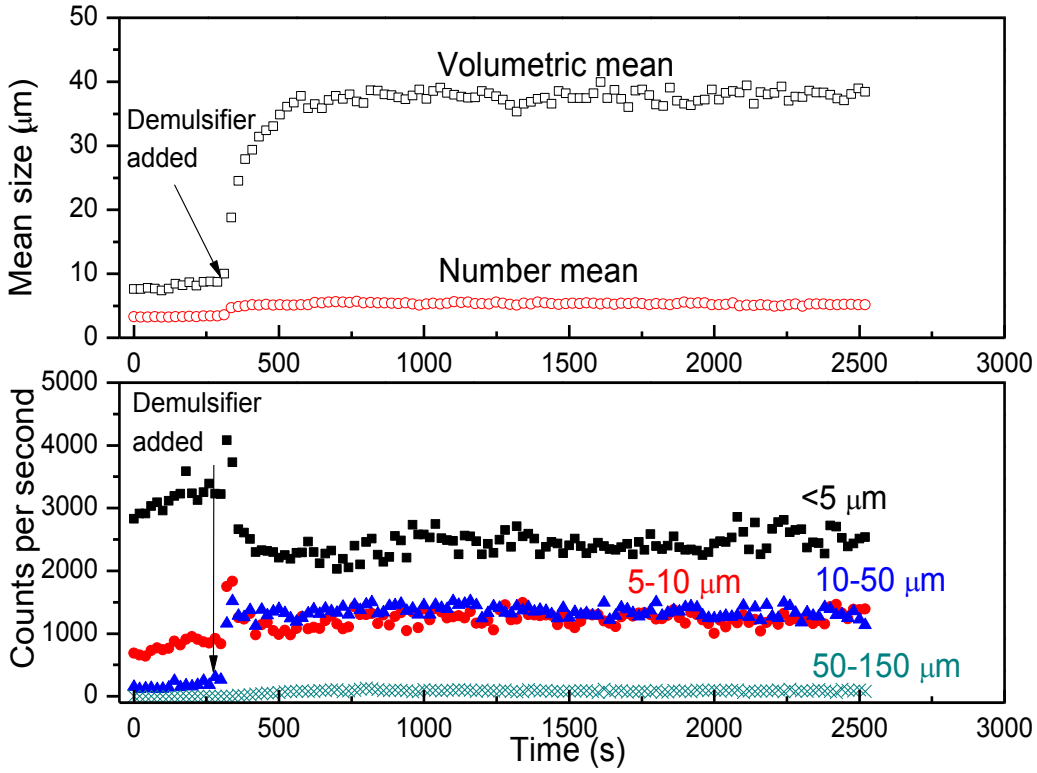

Figure 4.2.2-3 Mean sizes and counts of the emulsion water droplets during demulsification with the addition 50 ppm demulsifier B.

Figure 4.2.2-4 shows the volumetric mean based and the number mean based chord length distribution (CLD) of the emulsion sample after different time periods (0, 1, 2, 3, 5, 15 and 35 min) following the addition of 50 ppm of demulsifier B. The water droplet size increased rapidly over the first 180 s. The system equilibrated 5 min after the demulsifier addition.

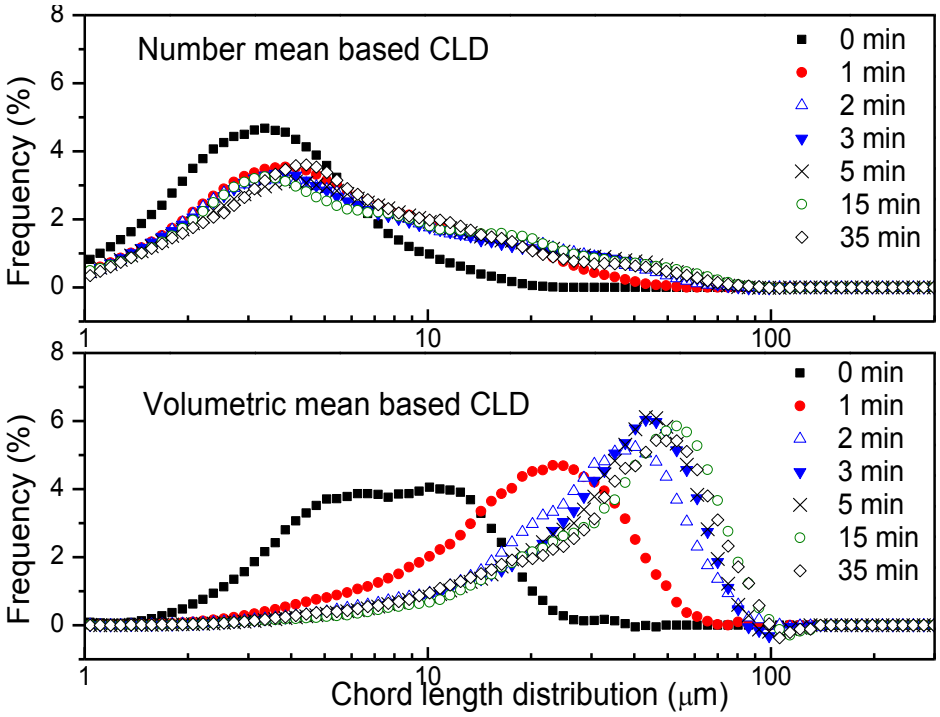

Figure 4.2.2-4 Chord length distribution of the emulsion water droplets during demulsification using 50 ppm demulsifier B at room temperature.

Figure 4.2.2-5 shows the micrographs of the emulsion water droplets before and after demulsification using 50 ppm demulsifier B at room temperature.

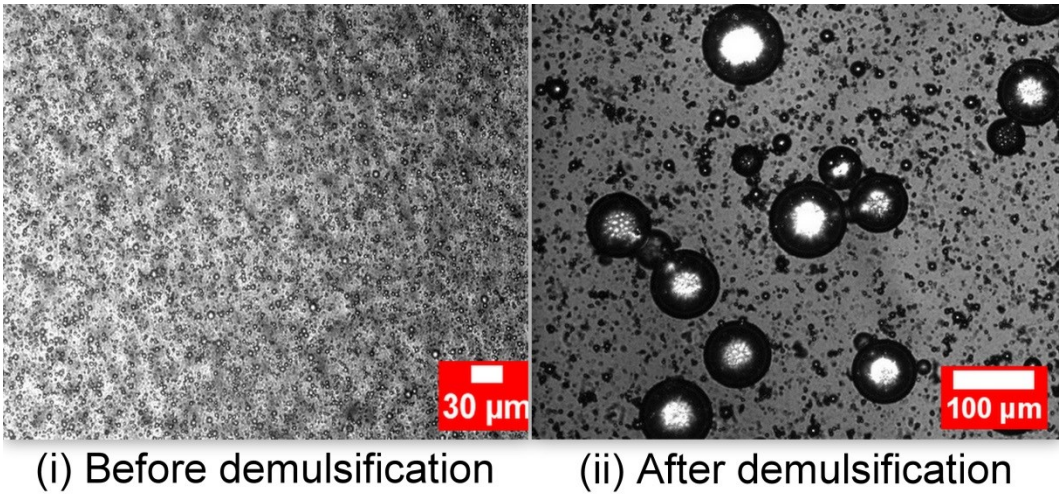

Figure 4.2.2-5 Morphology changes of the emulsion water droplets after demulsification with 50 ppm of demulsifier B at room temperature.

Before demulsification, most of the water droplets were smaller than 5 μm. After demulsifier was added, some droplets formed small flocs while others coalesced, forming large water droplets. The morphology changes upon demulsifier addition reveal that coalescence was the main mechanism responsible for water droplet size increase in the demulsification of 50 ppm demulsifier B at room temperature.

Software Image J was applied to determine the droplet size and calculate the water droplet diameter distribution of the emulsion sample before and after demulsification (as shown in Figure 4.2.2-5). More than 200 water droplets were used to calculate the emulsion water droplet diameter distribution in each case. The calculated water droplet diameter distribution before and after demulsification are shown in Figure 4.2.2-6.

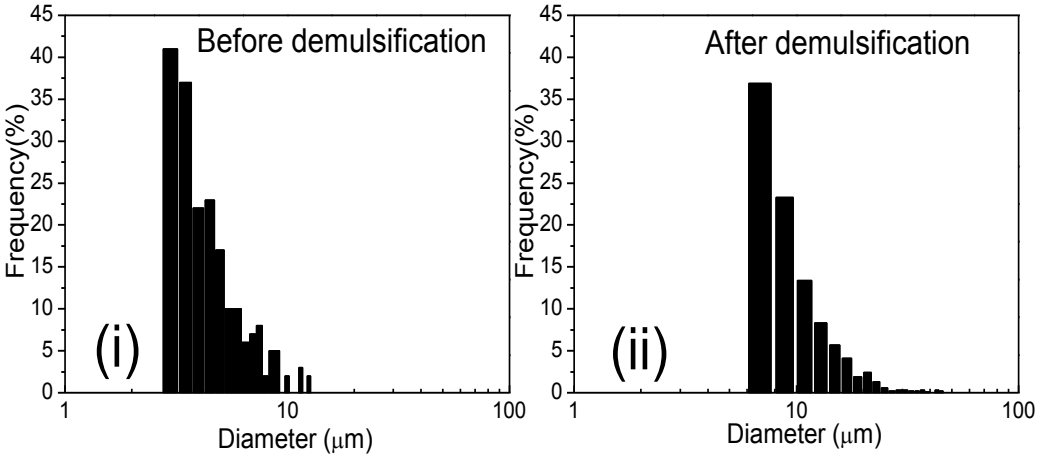

Figure 4.2.2-6 Calculated water droplet diameter distribution before and after demulsification using 50 ppm demulsifier B at room temperature.

The results show that the dominant size of water droplets before demulsifier addition was around 3 μm, whereas it increased to 7 μm after demulsifier addition with the addition of 50 ppm of demulsifier B. The droplet size distribution measured by the optical microscope is in good agreement with the number mean size measured using FBRM, demonstrating that the number mean represents well the water droplet size distribution of the emulsion sample. Compared with the calculated droplet size from image analysis, the volumetric mean size measured by FBRM was much bigger than the actual size of coalesced water droplets, though it can reflect the rapid size increase caused by the addition of demulsifier. The size changes reflected by the number mean were more close to the actual condition. Therefore in section 4.2.3-4.2.4, the water droplet size change is presented in terms of number mean.

4.2.3 Demulsification kinetics

Impact of demulsifier concentration and temperature

The kinetics of demulsification of PEO-PPO copolymers was observed by FBRM after adding the four demulsifiers into water-in-toluene diluted bitumen emulsions described in section 3.4.2. Various dosages of the demulsifiers were used to investigate the demulsifier concentration impact on the water droplet size increase, namely 10 ppm, 50 ppm and 100 ppm. The mean size of the water droplets before and after demulsifier addition at either room temperature or 60 °C is given in Figures 4.2.3-1 - 4.2.3-4 in the form of number mean. All tests were assured to be repeatable by conducting independent tests. The percent error of the measured number mean size of all cases was below 5 %.

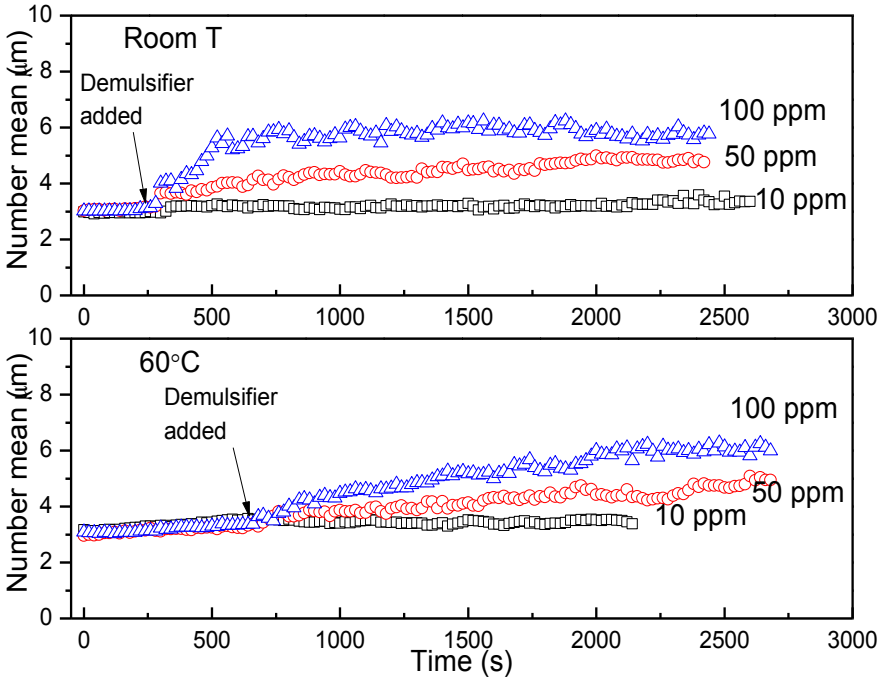

Figure 4.2.3-1 Number mean of the emulsion water droplets with addition of various concentrations of demulsifier A at room temperature and 60 ºC.

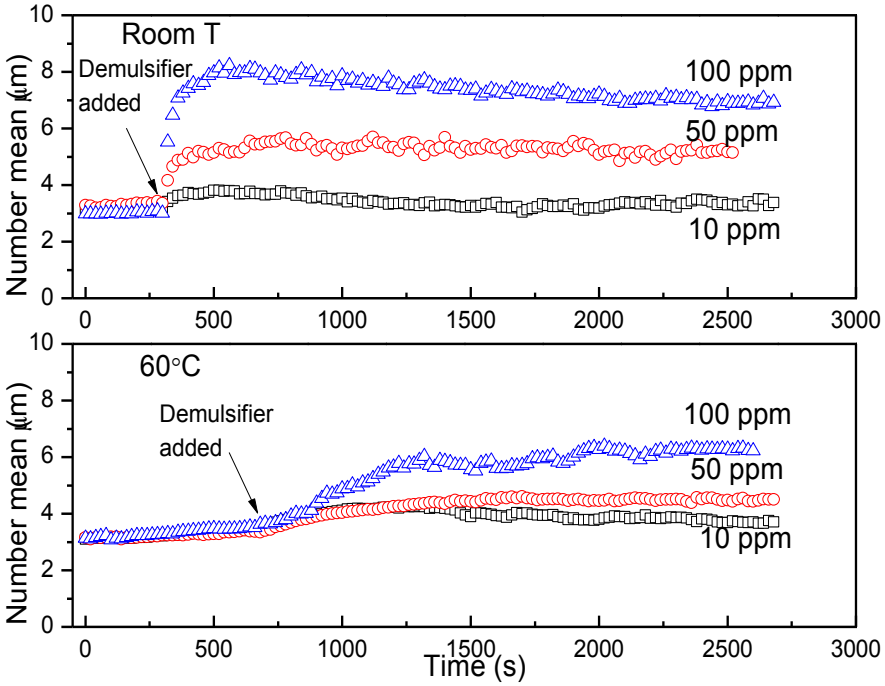

Figure 4.2.3-2 Number mean of the emulsion water droplets with addition of various concentrations of demulsifier B at room temperature and 60 ºC.

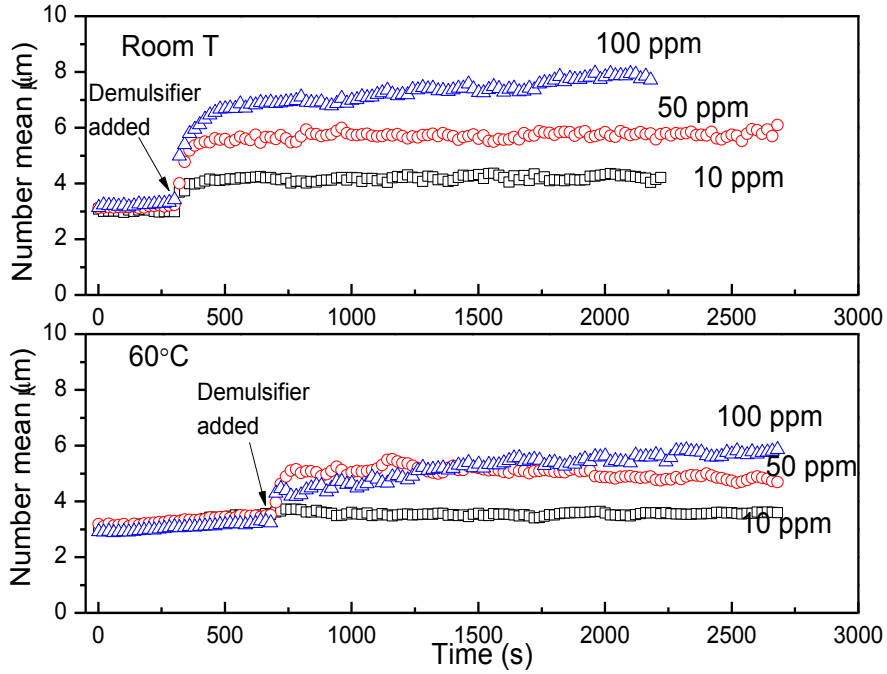

Figure 4.2.3-3 Number mean of the emulsion water droplets with addition of various concentrations of demulsifier C at room temperature and 60 ºC.

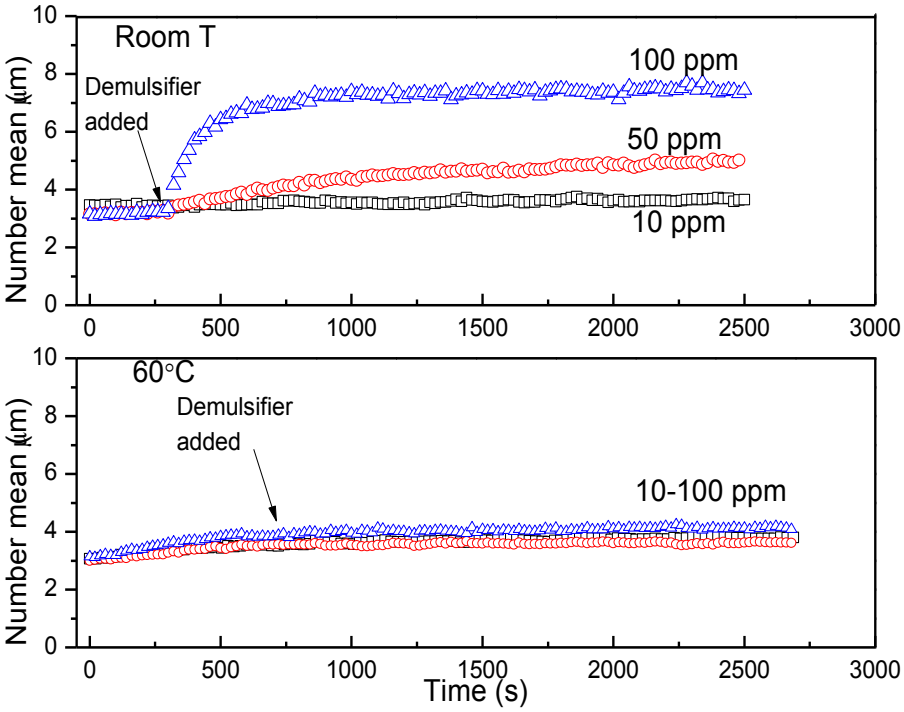

Figure 4.2.3-4 Number mean of the emulsion water droplets with addition of various concentrations of demulsifier D at room temperature and 60 ºC.

The data reveal that the emulsion water droplet size increase of the system upon addition of the four demulsifiers was dependent on the concentration of demulsifiers at either room temperature or 60 °C. The final number mean size in each test was influenced by demulsifier types as well. The increase in temperature decreased the final number mean size of the emulsion water droplets and the growth rate of water droplet number mean size. Key information about demulsification kinetics of each test including final number mean size and the time reaching the equilibration was determined and summarized in Table 4.2.3.

The final number mean size values shown in Table 4.2.3 were the average of the last 800 s number mean sizes of each test, respectively. It can be seen that the four demulsifiers increased the number mean size similarly at room temperature, despite their different properties, suggesting that chemical demulsification with the involvement of mixing is influenced more by demulsifier dosage rather than by demulsifier type. At 60 ^{o}C, the ability to increase water droplet size of demulsifier A, demulsifier B and demulsifier C was impacted slightly by temperature, where it took longer time for the system to equilibrate. Demulsifier D showed no size increase at 60 °C. It is worth nothing that demulsifier D is also the one whose interfacial activity was lowered by temperature increase. However, interfacial tension is not the sole factor influencing demulsification. The performance of the four demulsifiers in breaking W/O emulsions is further probed by bottle tests.

Table 4.2.3 Key parameters of the FBRM demulsification tests using the four PEO-PPO copolymers.

	Dosage (ppm)	Final size (μm, 25 °C)	Time reaching final size (s, 25 °C)	Final size (μm, 60 °C)	Time reaching final size (s, 60 °C)
A	10	3.16±0.05	---	3.45±0.04	---
	50	4.39±0.13	~500	4.42±0.13	~1350
	100	5.83±0.20	~250	5.91±0.22	~1350
B	10	3.27±0.08	~60	4.18±0.07	~350
	50	5.43±0.15	~350	4.48±0.06	~500
	100	7.73±0.22	~180	5.90±0.24	~500
C	10	4.14±0.06	~100	3.54±0.04	~150
	50	5.68±0.12	~110	5.17±0.16	~150
	100	7.58±0.23	~200	5.65±0.15	~900
D	10	3.54±0.04	---	3.67±0.05	---
	50	4.85±0.14	~750	3.58±0.05	---
	100	7.32±0.08	~250	3.81±0.04	---

Remaining water contents of the emulsion samples after FBRM demulsification were summarized in Figure 4.2.3-5. The data show that for the four PEO-PPO copolymers, demulsification at 60 ^{o}C produced better water removal effect than at room temperature conditions. Without the addition of demulsifiers, the remaining water content of the blank emulsion sample was reduced to below 4% after the FBRM test. Similar trends were found in the cases using demulsifiers A, C and D at 60 ^{o}C. For demulsifier B, the improvement on water removal at higher

temperature was observed at 10 ppm. At higher dosages, since the remaining water content of the samples were fairly low at room temperature, the enhancement on water removal efficiency at high temperature was difficult to be detected.

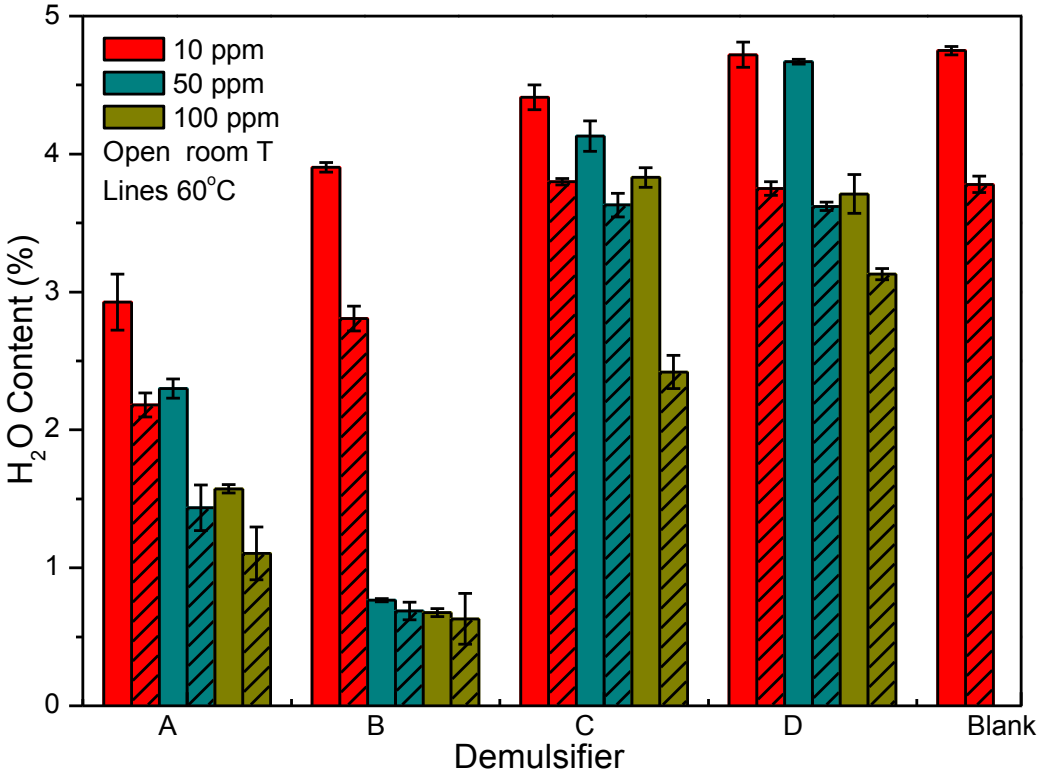

Figure 4.2.3-5 Remaining water content of the emulsion after FBRM demulsification.

Demulsification mechanisms of the four demulsifiers

The size increase of emulsion water droplets during demulsification can be achieved by coalescence and flocculation. It is determined by the properties of the demulsifier to have coalescence or flocculation to occur. The present section aims to probe the demulsification mechanisms of the four demulsifiers. Figures 4.2.3-6 - 4.2.3-9 show the micrographs of the emulsion 2 min after demulsification tests.

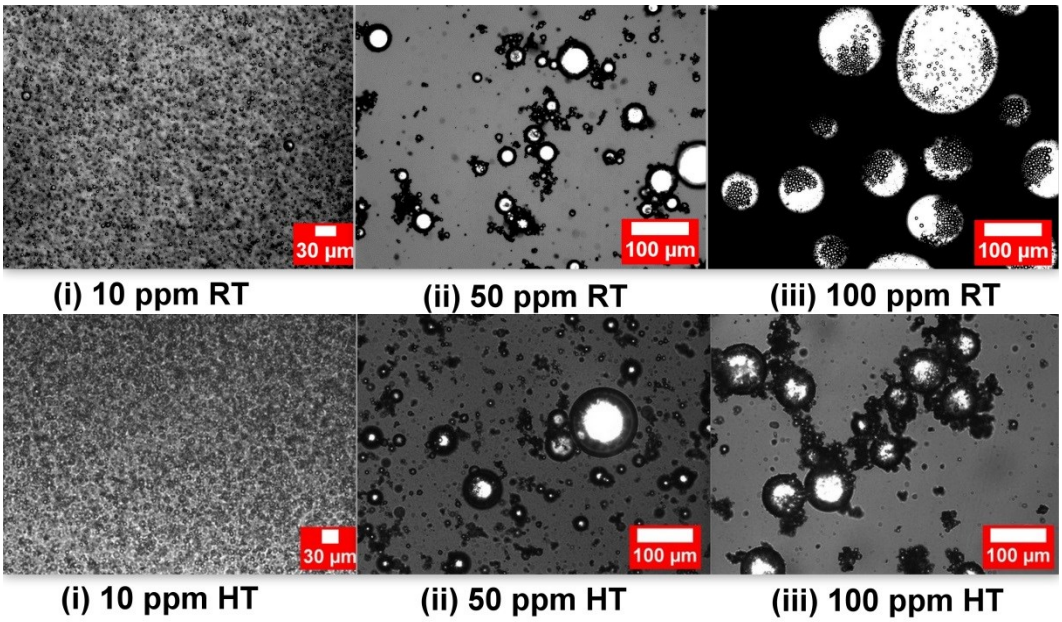

Figure 4.2.3-6 Morphology of the emulsion water droplets after demulsification with various concentrations of demulsifier A. (RT: room temperature; HT: 60 °C)

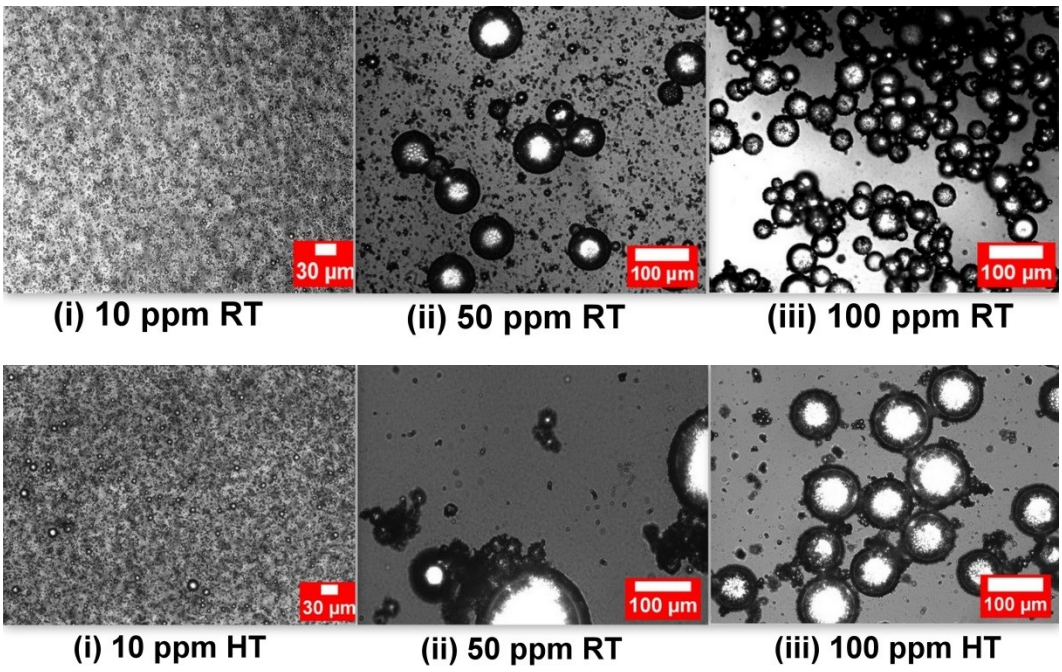

Figure 4.2.3-7 Morphology of the emulsion water droplets after demulsification with various concentrations of demulsifier A. (RT: room temperature; HT: 60 °C)

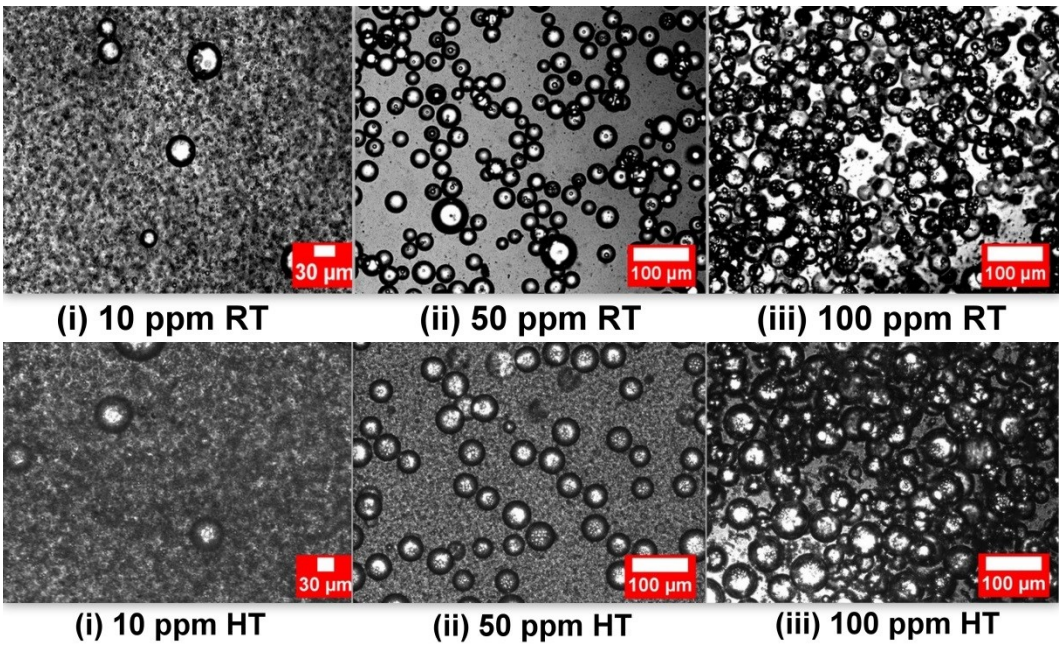

Figure 4.2.3-8 Morphology of the emulsion water droplets after demulsification with various concentrations of demulsifier A. (RT: room temperature; HT: 60 °C)

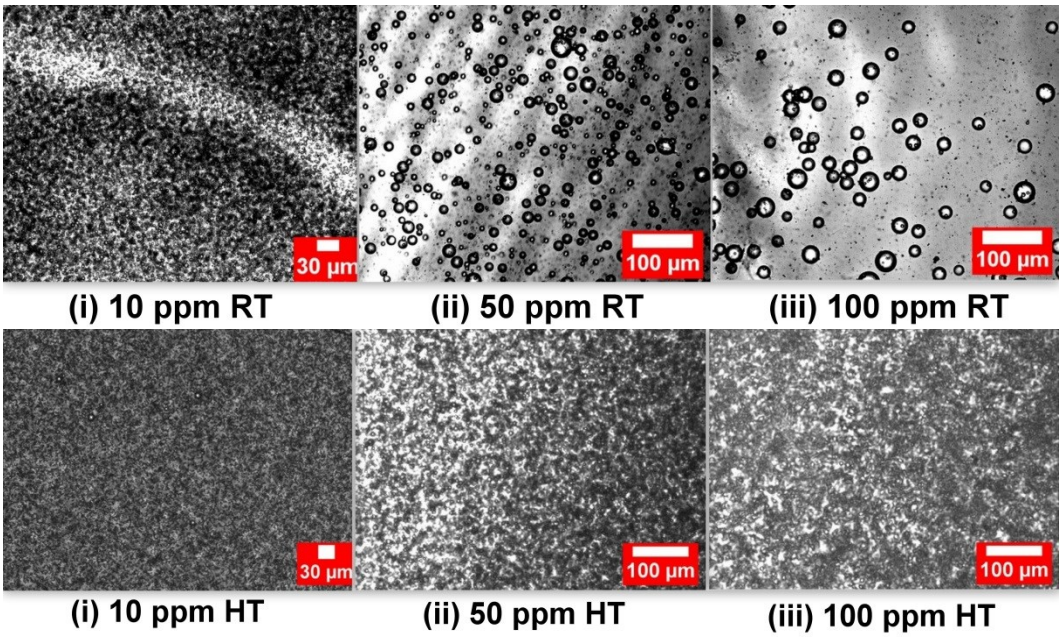

Figure 4.2.3-9 Morphology of the emulsion water droplets after demulsification with various concentrations of demulsifier A. (RT: room temperature; HT: 60 °C)

Flocs were clearly observed in micrographs of the emulsion samples broken by demulsifier A and demulsifier B, in which clusters of small water droplets were seen sticking together, forming large coalesced water droplets. This finding indicates that both coalescence and flocculation contributed to increasing water droplet size in these two cases. Conversely, the clear edges of the water droplets in the emulsions broken by demulsifier C and demulsifier D reveal that coalescence is the main contributor for water droplet size increase. Since demulsifiers with large molecular weight are known to be good flocculants, the fact that demulsifier A and demulsifier B were able to induce flocculation is probably owing to their relatively large molecular weight, which are 12,311 Dalton (demulsifier A) and 10,003 Dalton (demulsifier B) [85 - 86].

4.3 Evaluation of the four demulsifiers in a static condition

4.3.1 Understanding bottle tests data of the four demulsifiers

Figure 4.3.1-1 shows the water content of the samples after 1 h of gravity settling at room temperature after adding each of the four demulsifiers at different dosages. The water content measured for the blank samples without demulsifier added is also given for comparison.

Blending time shown in Figure 4.3.1-1 is the time used to blend demulsifier solution with an emulsion sample at 300 rpm before gravity settling. The data reveal that in the absence of demulsifiers, the water-in-toluene diluted bitumen emulsions were rather stable having insignificant changes in water content with up to 5 min of blending after 1 h settling.

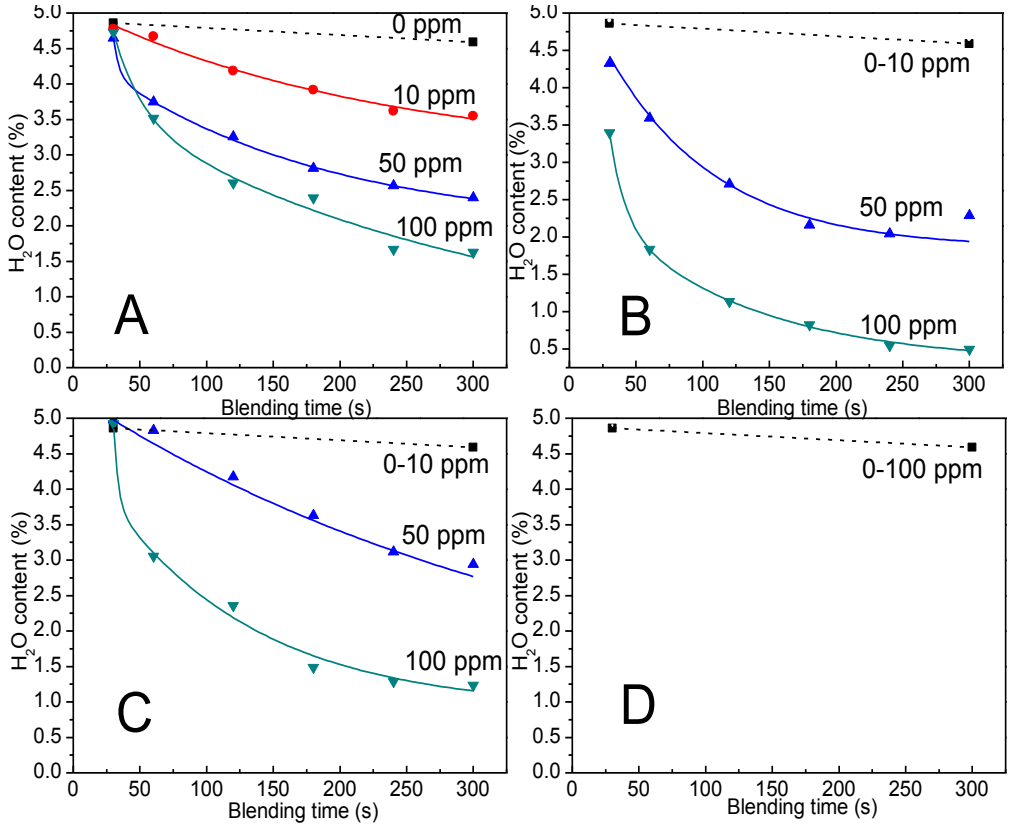

Figure 4.3.1-1 Water content of the emulsion samples after bottle test using different dosages of the four demulsifiers at room temperature as a function of blending time.

The data further show that when demulsifiers were added, the water content in the oil phase of the emulsion samples was most effectively reduced at high demulsifier concentration and when the demulsifier was blended for a sufficiently long period of time. Blending time is an important factor because the migration of demulsifier molecules to the bitumen-water interface can be accelerated by mixing [6]. As shown in Figure 4.3.1-1, with blending time increased to 5 min, remaining water content of the emulsion samples tended to be constant. This finding indicates that 5-min blending at 300 rpm was sufficient to ensure that the demulsifier molecules diffuse well in the emulsions. On the basis of these results,

bottle tests conducted to probe the effect of demulsifier dosage and type on dewatering efficiency were investigated with the bottle tests' data under 5 min blending time.

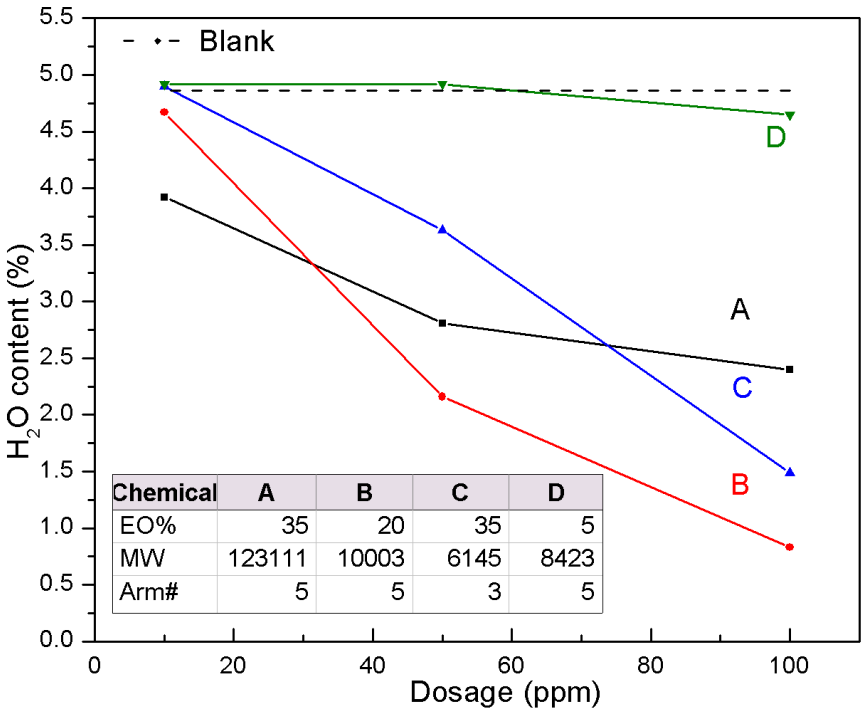

Chemical	A	B	C	D
EO%	35	20	35	5
MW	123111	10003	6145	8423
Arm#	5	5	3	5

Figure 4.3.1-2. The impact of demulsifier type on dewatering efficiency.

Figure 4.3.1-2 shows that the addition of the four demulsifiers led to various remaining water contents of the emulsion samples after 1 h gravity settling. Demulsifier B seemed to be the most effective in reducing residual water level of the sample at 50 ppm and 100 ppm of demulsifier dosages. Among the four demulsifiers, at 10 ppm demulsifier A lowered the water content of the emulsion upper phase the most. The data also show that the performance of demulsifiers A, B and C was concentration dependent, with the highest dosage yielding the best dewatering performance. Conversely, demulsifier D had limited ability to resolve

the emulsified water present in the diluted bitumen phase. The possible factors determining the performance of the four demulsifiers are discussed in the following section.

4.3.2 Influence of the demulsifiers' characteristics

The present section discusses the possible correlations between dewatering performance and the important properties of the demulsifiers, including amphiphilicity, molecular weight and affinity to the oil-water interface of the demulsifiers.

Hydrophilic-lipophilic balance and dewatering efficiency

The correlation between RSN and dewatering performance of the four PEO-PPO copolymers is given in Figure 4.3.2-1.

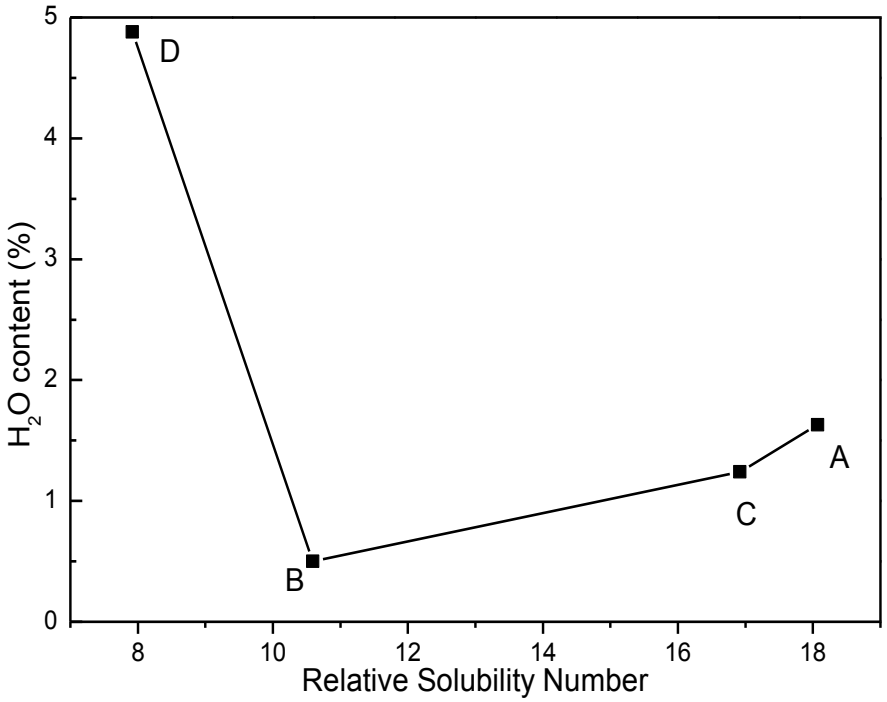

Figure 4.3.2-1 Dewatering results of the four demulsifiers at 100 ppm as a function of RSN.

It is evident that of all demulsifiers, the one with an RSN value of 10.59 (demulsifier B) had the best dewatering performance, whereas demulsifiers with an RSN values above or below this value were not as effective in reducing the water content of the emulsions. These results suggest that an appropriate balance between EO and PO groups is important for obtaining a good demulsification performance, although caution should be exercised when interpreting the obtained results since the demulsifiers used differ in more than one parameter. Previous research reported that the correlation between hydrophilic-lipophilic balance of demulsifiers and their dewatering effect: Xu *et al.* [52] reported that dewatering of W/O emulsions is dependent on the demulsifier's relative solubility number (RSN). However, only within a given PEO-PPO copolymers family, can an optimum RSN range be observed. Xu [87] also reported that when EO% is close to its PO%, the PEO-PPO demulsifier is more effective in dewatering than demulsifies of EO%>>PO% or EO%<<PO%. Fan and Sjöblom *et al.* [88] studied the dewatering performance of a series of polyoxyethylene (water-liking) nonphenols (oil-liking) demulsifiers with different HLB. They found that demulsifiers in a same family with lower/higher HLB than an optimum value performed less effectively than the one having the optimum HLB. Schramm *et al.* [50] claimed that commercial demulsifiers with relatively high HLB values (15-20) effectively reduced residual water content without affecting oil recovery. Pereira *et al.* [51] showed the negative impact of strong hydrophilicity of a demulsifier in dewatering. Al-Sabagh *et al.* [49] claimed that an intermediate

EO/PO content gave the best demulsification efficiency. In conclusion, strong hydrophilicity/hydrophobicity of a demulsifier could cause detrimental effects for demulsification. The optimum RSN of a series of demulsifiers for breaking a certain emulsion is determined by demulsifiers' properties and the characteristics of the emulsion.

Impact of molecular weight of demulsifiers on demulsification

Large molecular weight is reported to improve dewatering performance of demulsifiers [52] [89]. Demulsifiers with high molecular weight are capable of bridging water droplets and binding them in close contact, thus promoting coalescence. A study done by Ese *et al.* [90] proved that demulsifiers with large molecular weight can increase the compressibility of asphaltenes-water interface more effectively than demulsifiers of small molecular weight. However, long alkyl chains may impede the adsorption of demulsifier molecules at oil-water interface due to steric effect [49].

In this context, the fact that demulsifier B has the best demulsification performance can be explained as a result of its high molecular weight and its balanced RSN. Demulsifier A and demulsifier C have similar RSN but very different molecular weight (demulsifier A of 12,311 Dalton vs demulsifier C of 6,145 Dalton). At 100 ppm, demulsifier A and demulsifier C had similar dewatering performance, but at 10 ppm, demulsifier A reduced water content to 3.55% in contrast to demulsifier C which reduced water content to 4.67%. The difference in the molecular weight of the two demulsifiers explains why demulsifier A performed better than demulsifier C at low dosages.

Affinity to oil-water interface and dewatering

Figure 4.3.2-2 shows the relationship between interfacial tension and dewatering results by the four demulsifiers at room temperature.

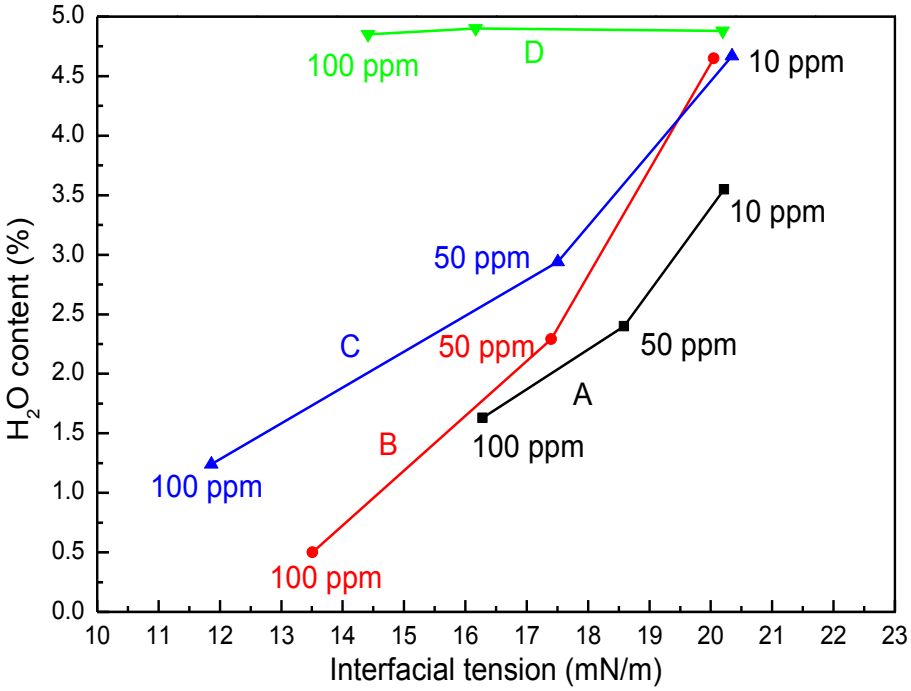

Figure 4.3.2-2 Dewatering vs interfacial tension at room temperature.

Figure 4.3.2-2 shows that the dewatering performance of demulsifiers A, B and C, deteriorated with increasing interfacial tension, suggesting that low interfacial tension condition promotes dewatering. Demulsifier D reduced interfacial tension as much as the other three demulsifiers at the concentrations tested (10 ppm, 50 ppm and 100 ppm). However, no noticeable dewatering effect was observed for the sample using demulsifier D, showing that interfacial tension is not the sole parameter controlling dewatering performance. This finding is in agreement with previous studies (Kailey *et al.*v [82] and Zaki *et al.* [91]). In addition to interfacial

tension, other factors including film pressure and demulsifier molecule arrangement at interface also impact demulsification efficiency tremendously [87] [92].

4.3.3 Impact of temperature on bottle tests

Figure 4.3.3 compares the amount of water resolved at room temperature and at 60ºC with each of the four demulsifiers tested.

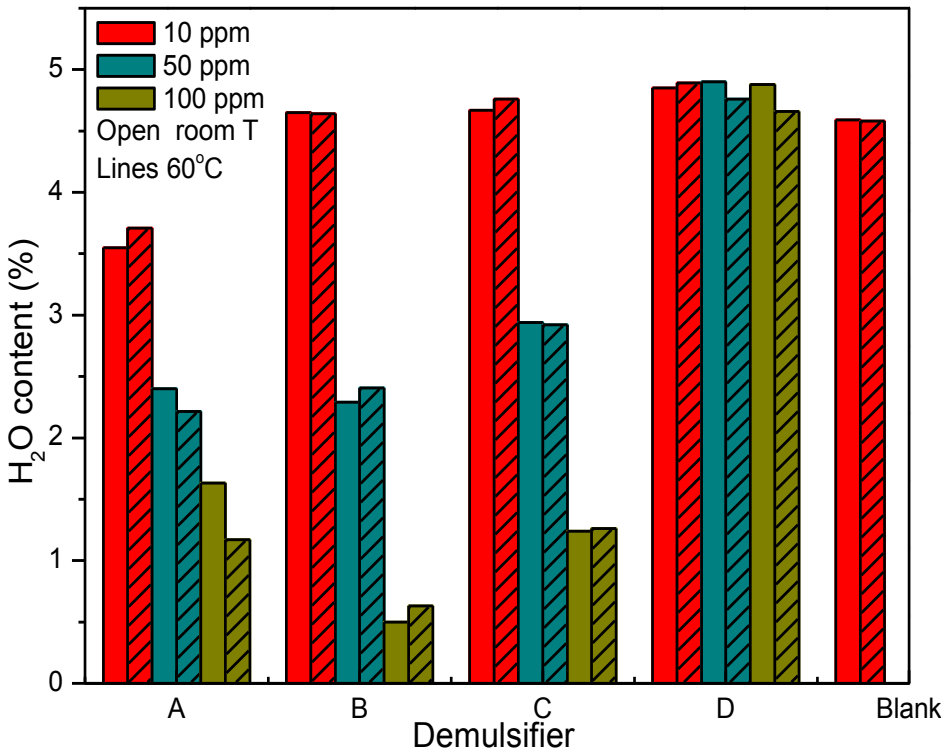

Figure 4.3.3 Dewatering results at room temperature and 60 ºC.

Figure 4.3.3 shows that increasing temperature from room temperature to 60 ºC does not impact dewatering in a significant manner for the four demulsifiers. The only case showing improvement is the test using 100 ppm of demulsifier A, for which the remaining water content was reduced from 1.63% at room temperature

to 1.17% at 60 °C. Demulsifier D is the only one whose affinity to interface became lower when changing the temperature from room temperature to 60 °C. Therefore it is expected to see the decrease in its ability to resolve the emulsified water in the emulsion. Since the performance of demulsifier D was very poor even at room temperature, no significant difference could be detected upon an increase in temperature from room temperature to 60 °C.

To better understand the temperature impact on bottle tests results, the viscosity of the diluted bitumen at room temperature and 60 °C were measured and presented in Table 4.3.

Table 4.3 Viscosity of solids free diluted bitumen at 25° C and 60° C.

Temperature/°C	25	60
Viscosity/mPa•s	27.81	11.71

Room temperature viscosity of the diluted bitumen in this work is quite low, much lower than that of crude bitumen (10^5 - 10^6 mPa·s). Due to the low viscosity of the sample at room temperature, probably the improvement of demulsification efficiency at increased temperature is not considerably obvious in bottle tests. Similar findings were reported by Yarranton *et al.* [59]. The authors reported that when toluene was used as solvent to conduct froth treatment at S/B=0.61, viscosity of the diluted bitumen was fairly low at 23 °C (9.8 mPa·s). When the sample temperature increased to 60 °C, although the viscosity of the continuous phase was reduced to less than a half of the viscosity of room temperature (4.4

mPa·s), the water content in the collected bitumen at high temperature was not significantly reduced as compared with the water content in the bitumen collected at room temperature. Essentially, the settling time used in the bottle tests was sufficiently long, which probably allowed that the settling of water droplets at room temperature achieved similar efficiency as it was at 60 °C within the tested period.

Chapter 5 Conclusions and Future Work

Four PEO-PPO copolymers were applied to break water-in-toluene diluted bitumen emulsions. The affinity to diluted bitumen-water interface of the four copolymers was evaluated by interfacial tension measurements in the presence/absence of the four demulsifiers. The demulsification performance of the four copolymers was investigated by FBRM and bottle tests. The impact of demulsifier concentration, mixing intensity and temperature on demulsification performance was studied. Viscosity of the diluted bitumen was measured at room temperature and elevated temperature in order to determine the impact of temperature on demulsification.

Interfacial tension measurements reveal that the four demulsifiers can effectively reduce the interfacial tension of the diluted bitumen-water interface. The performance of the four demulsifiers in reducing interfacial tension was dependent on demulsifier concentration. Demulsifiers with high EO% (demulsifier A and demulsifier C) were more effective in reducing interfacial tension than demulsifiers of less EO% (demulsifier B and demulsifier D). At 60 ^{o} C, the interfacial activity of demulsifier D was lowered to a certain degree, possibly as a result of conformational changes of demulsifier D at high temperature. Dynamic interfacial tension data led to similar conclusions on the impact of hydrophilicity of demulsifiers in reducing interfacial tension. Additionally, the systems containing demulsifiers of relatively lower molecular weight (demulsifiers C, D) took shorter time to equilibrate as compared with

systems containing large molecular weight demulsifiers (demulsifier A and demulsifier B).

FBRM demulsification tests showed that the demulsification using the four PEO-PPO copolymers was influenced the most by mixing condition and demulsifier concentration. The optimum stirring speed for demulsification was determined to be 220 rpm, whereas larger or smaller stirring speeds could not ensure satisfying demulsification performance. The size of emulsion water droplets after demulsification was the biggest when 100 ppm (highest concentration) of demulsifier was added. However, the structure of demulsifiers also played a role in determining the final size of coalesced water droplets. At 60 ^{o}C, demulsifier D did not induce coalescence or flocculation to increase the emulsion water droplet size, whereas the other three demulsifiers all effectively increased water droplet size. In addition, the growth rate of the emulsion water droplet was slower at 60 ^{o} C than at room temperature.

Bottle test results revealed that the dewatering abilities of the four demulsifiers. Blending time of 5 min was determined to be sufficient to evaluate the dewatering efficiency of the demulsifiers. Bottle test results showed that the demulsifier with intermediate RSN (demulsifier B) produced the best dewatering performance among the four demulsifiers, whereas demulsifiers with higher or lower RSN (demulsifiers A, C and D) did not resolve the emulsions as effectively. Though demulsifier D was able to reduce the interfacial tension of the diluted bitumen-water interface effectively, its negligible effect on lowering the water content of

the oil phase in the emulsions proved that interfacial tension condition is not the sole parameter influencing dewatering of the water-in-diluted bitumen emulsions.

The performance of all the demulsifiers except demulsifier D in both FBRM demulsification tests and bottle tests was not significantly impacted by temperature. The main effect of the temperature increase from room temperature to 60 °C was to lower the viscosity of continuous phase of the emulsions. In FBRM tests, the fact that increasing temperature from room temperature to 60 °C did not induce significant improvement on water droplet size increase while water removal efficiency is seen to increase proves that the FBRM tests provide a powerful means to distinguish the enhanced demulsification mechanisms by demulsifier addition at high temperature operations. Clearly increasing temperature did not render enhanced flocculation and/or coalescence of emulsified water droplets.

For the bottle tests, the viscosity reduction was supposed to further reduce the remaining water content of the emulsion samples at elevated temperature. The failure to observe such a phenomenon in the bottle tests was probably caused by the over-long settling time used in the tests, which was too long to differentiate the demulsification efficiency of the demulsifiers at room temperature and elevated temperature with respect to dewatering rate.

Finally, it is proved that the demulsification performance of PEO-PPO copolymers is correlated to their amphiphilicity at both room temperature and high temperature. Demulsifiers with relatively large molecular weight

(demulsifiers A and B) achieved better demulsification effects compared to demulsifiers with smaller molecular weight (demulsifiers C and D). Demulsifiers A and D flocculated the emulsion water droplets during demulsification owing to their relatively large molecular weight, as observed in FBRM demulsification tests.

Future Work

Bottle tests and interfacial tension measurements illustrate that demulsifier D reduced interfacial tension effectively at tested dosages but failed to reduce the water content of the emulsion samples. To investigate why demulsifier D could not break the W/O emulsions, interfacial film properties in the presence of demulsifier D should be probed. Techniques including Langmuir trough, Thin Film Balance and/or AFM may be useful for such purposes.

It is worth to investigate the temperature impact on dewatering efficiency in bottle tests by measuring the remaining water percentage of the emulsion samples as a function of time at fixed demulsifiers' concentrations.

Additionally, temperature increase would inevitably increase the system pressure if the demulsification is conducted in a closed vessel. It is of interest to investigate the impact of pressure change on the demulsification of the W/O emulsions.

References

[1] "Canada's Oil Sands: A supply and Market Outlook to 2015," Board of National Energy, 2000.

[2] A. Government, "Alberta Energy: Facts & Statistics," Statistics Canada and Alberta Treasury Board and Finance, 2014. [Online]. Available: http://www.energy.alberta.ca/OilSands/791.asp.

[3] J. Masliyah, Z. Zhou, Z. Xu, J. Czarnecki and H. Hamza, "Understanding Water-Based Bitumen Extraction from Athabasca Oil Sands," *The Canadian Journal of Chemical Engineering,* vol. 82, pp. 628-654, 2004.

[4] J. H. Masliyah, J. Czarnecki and Z. Xu, "Introduction to the Athabasca Oil Sands," in *Handbook on Theory and Practice of Bitumen Recovery from Athabasca Oil Sands*, Edmonton, Kingsley Knowledge Publishing, 2011, pp. 1-51.

[5] Z. Xu, "Bitumen Production from Canadian Oil Sands Deposits," in *AICHE Annual Meeting*, 2007.

[6] J. H. Masliyah, J. Czarnecki and Z. Xu, "Froth Treatment Fundamentals," in *Handbook on Theory and Practice of Bitumen Recovery from Athabasca Oil Sands*, Edmonton, Kingsley Knowledge Publishing, 2011, pp. 349-386.

[7] S. C. Pandey, D. K. Ralli, A. K. Saxena and W. K. Alamkhan, "Physicochemical Characterization and Application of Naphtha," *Journal of*

Scientific & Industrial Research, vol. 63, pp. 276-282, 2004.

[8] R. Tipman, "Froth Treatment," in *Handbook on Theory and Practice of Bitumen Recovery from Athabasca Oil Sands Vol II*, Edmonton, Kingsley Knowledge Publishing, 2013, pp. 211-250.

[9] Y. Long, T. Dabros and H. Hamza, "Stability and Settling Characteristics of Solvent-Diluted Bitumen Emulsions," *Fuel,* vol. 81, pp. 1945-1952, 2002.

[10] M. Phukan, K. Koczo, B. Falk and A. Palumbo, "New Silicone Copolymers for Efficient Demulsification," in *SPE Oil and Gas India Conference and Exhibition*, Mumbai, 2010.

[11] D. Nguyen, N. Sadeghi and C. Houston, "Chemical Interactions & Demulsifier Characteristics for Enhanced Oil Recovery Applications," *Energy & Fuels,* vol. 26, pp. 2742-2750, 2012.

[12] Y. Xu, J. Wu, T. Dabros and H. Hamza, "Optimizing the Polyethylene Oxide and Polypropylene Oxide Contents in Diethylenetriamine-Based Surfactants for Destabilizing of a Water-in-Oil Emulsions," *Engergy & Fuel,* vol. 19, pp. 916-921, 2005.

[13] Y. Xu, J. Wu, T. Dabros, H. Hamza, S. Wang, M. Bidal and J. Venter, "Breaking Water-in-Bitumen Emulsions useing Polyoxyalkylated DETA Demulsifiers," *CAN J CHEM ENG,* vol. 82, pp. 829-835, 2004.

[14] Z. Zhang, G. Xu, F. Wang, S. Dong and Y. Chen, "Demulsification by Amphiphilic Dendrimer Copolymers," *Journal of Colloid and Interface Science,* vol. 282, pp. 1-4, 2005.

[15] W. E. Shelfantook, "A Perspective on the Selection of Froth Treatment Processes," *The Canadian of Chemical Engineering,* vol. 82, pp. 704-709, 2004.

[16] B. Xu, W. Wang and L. Meng, "Influence of Water Content and Temperature on Stability of W/O Crude Emulsions," *Petroleum Science and Technology,* vol. 31, pp. 1099-1108, 2013.

[17] A. M. Al-Sabagh, N. M. Nasser, M. El-Sukkary, A. Eissa and T. Abd El-Hamid, "Demulsification Efficiency of Some New Stearate Esters of Ethoxylated & Propoxylated 1,8-Diamino-Octane for Water-in-Crude Oil Emulsions," *Journal of Dispersion Science & Technology,* vol. 34, pp. 1409-1420, 2013.

[18] J. Dufour, . J. A. Calles, J. Marugan, R. Gimenez-Aguirre, J. L. Pena and D. Merino-Garcia, "Influence of Hydrocarbon Distribution in Crude Oil & Residues on Asphaltene Stability," *Energy & Fuels,* vol. 24, pp. 2281-2286, 2010.

[19] J. A. Boxall, C. A. Koh, E. D. Sloan, A. K. Sum and D. T. Wu, "Droplet Size Scaling of Water-in-Oil Emulsions under Turbulent Flow," *Langmuir,* vol.

28, pp. 104-110, 2012.

[20] J. A. Boxall, C. A. Koh, E. Dendy Sloan, A. K. Sum and D. T. Wu, "Measurement and calibration of Droplet Size Distribution in Water-in-Oil Emulsions by Particle Video Microscope and a Focused Beam Reflectance Method," *Ind. Eng. Chem. Res.,* vol. 49, pp. 1412-1418, 2010.

[21] S. Less, R. Vilagines and H. Al-Khalifa, "Online Droplet Diameter Measurements to Improve the Crude Oil Dehydration Process," *Chem. Eng. Res. Des,* p. In Press, 2014.

[22] A. K. Mehrotra, R. R. Eastick and W. T. Svrcek, "Viscosity of Cold Lake Bitumen and Its Fraction," *The Canadian Journal of Chemical Engineering,* vol. 67, pp. 1004-1009, 1989.

[23] C. Jiang, B. Bennett, S. Larter, J. Adams and L. Snowdon, "Viscosity and API Gravity Determination of Solvent Extracted Heavy Oil and Bitumen," *Journal of Canadian Petroleum Technology,* vol. 49, pp. 20-27, 2010.

[24] J. Guan, M. Kariznovi, H. Nourozieh and J. Abedi, "Density and Viscosity for Mixtures of Athabasca Bitumen and Aromatic Solvents," *Journal of chemical&Engineering data,* vol. 58, pp. 611-624, 2013.

[25] O. Strausz and E. Lown, The chemistry of the Alberta oil sands bitumens and heavy oils, Calgary: Alberta Energy Research Institute, 2003.

[26] J. H. Masliyah, J. Czarnecki and Z. Xu, "Physical and Chemical Properties of Oil Sands," in *Handbook on Theory and Practice of Bitumen Recovery from Athabasca Oil Sands*, Edmonton, Kingsley Knowledge Publishing, 2011, pp. 173-267.

[27] J. Czarnecki, B. Radoev, L. L. Schramm and R. Slavchev, "On the Nature of Athabasca Oil Sands," *Adv. Colloid. Interfac.,* vol. 114, pp. 53-60, 2005.

[28] T. Fan, J. Wang and J. S. Buckley, "Evaluation Crude Oils by SARA Analysis," in *SPE/DOE Improved Oil Recovery Symposium*, Tulsa, 2002.

[29] H. E. Gunning and J. K. Liu, Syncrude Analytical Methods Manual for Bitumen Upgrading, Edmonton: Alberta Oil Sands Technology and Research Authoriy, 1991.

[30] D. Thomas, H. Becker and R. Del Real Soria, "Controlling Asphaltene Deposition in Oil Wells," *SPE Production and Facilities,* vol. 10, pp. 119-123, 1995.

[31] F. J. Nellensteyn, In the Science of Petroleum, New York: Oxford University , 938.

[32] H. W. Yarranton, H. Alboudwarej and R. Jakher, "Investigation of Asphaltene Association with Vapor Pressure Osmometry and Interfacial Tension Measurements," *Industrial & Engineering Chemistry Research,* vol. 39, pp. 2916-2924, 2000.

[33] A. Sharma and O. Mullins, "Insights into molecular and Aggregate Structures of Asphaltenes Using HRTEM," in *Asphaltenes, heavy oils and petroleomics*, New York, Springer, 2007, pp. 205-229.

[34] J. Czarnecki, P. Tchoukov, T. Dabros and Z. Xu, "Role of Asphaltenes in Stabilisation of Water in Crude Oil Emulsions," *Can. J. Chem. Eng.,* vol. 91, pp. 1365-1371, 2013.

[35] J. C. Berg, "Emulsions and Foams," in *An Introduction to Interface & Colloids The Bridge to Nanoscience*, Danvers, World Scientific Publishing, 2010, pp. 643-691.

[36] X. Wu, T. van de Ven and J. Czarnecki, "Colloidal Forces between Emulsified Water Droplets in Toluene-Diluted Bitumen," *Colloid Surf. A,* vol. 149, pp. 577-583, 1999.

[37] A. Yeung, T. Dabros, J. Masliyah and J. Czarnecki, "Micropipette: A New Technique in Emulsion Research," *Colloids and Surfaces A: Physicochem. Eng. Aspects,* vol. 174, pp. 169-181, 2000.

[38] T. Dabros, A. Yeung, J. Masliyah and J. Czarnecki, "Emulsification through Area Contraction," *Journal of Colloid and Interface Science,* vol. 210, pp. 222-224, 1999.

[39] X. Yang and J. Czarnecki, "The Effect of Naphtha to Bitumen Ratio on Properties of Water in Diluted Bitumen Emulsions," *Colloid. Surf. A,* vol.

211, pp. 213-222, 2002.

[40] X. Wu, "Investigating the Stability Mechanism of Water-in-Diluted Bitumen Emulsions through Isolation and Characterization of the Stabilizing Materials at the Interface," *Energy & Fuels,* vol. 17, pp. 179-190, 2003.

[41] J. Czarnecki, "Stabilization of Wate in Crude Oil Emulsion. Part 2," *Energy & Fuels,* vol. 23, pp. 1253-1257, 2009.

[42] J. Czarnecki and K. Moran, "On the Stabilization Mechanism of Water-in-Oil Emulsions in Petroleum Systems," *Energy & Fuels,* vol. 19, pp. 2074-2079, 2005.

[43] Y. Fan, S. Simon and S. Johan, "Influence of Nonionic Surfactants on the Surface and Interfacial Film Properties of Asphaltenes Investigated by Langmuir Balance and Brewster Angle Microscopy," *Langmuir,* vol. 26, pp. 10497-10505, 2010.

[44] J. Davies and E. Rideal, Interfacial Phenomena, 2nd edn, New York: Academic Press, 1963.

[45] J. H. Masliyah, J. Czarnecki and Z. Xu, "Basic Scientific Background," in *Handbook on Theory and Practice of Bitumen Recovery from Athabasca Oil Sands*, Edmonton, Kingsley Knowledge Publishing, 2011, pp. 51-125.

[46] W. Griffin, "Classification of Surface-active agents by HLB," *Journal of the*

Society of Cosmetic Chemists, vol. 1, pp. 311-326, 1949.

[47] H. L. Greenwald, G. L. Brown and M. N. Fineman, "Determination of Hydrophile-Lipophile Character of Surface Active Agents and Oils by Water Titration," *Analytical Chemistry,* vol. 28, pp. 1693-1697, 1956.

[48] J. Wu, Y. Xu, T. Dabros and H. Hamza, "Development of a Method for Measurement of Relative Solubility of Nonionic Surfactants," *Colloids and Surfaces A: Physicochem. Eng. Aspects,* vol. 232, pp. 229-237, 2004.

[49] A. Al-Sabagh, M. N. El-Din, S. A.-E. Fotouh and N. Nasser, "Investigation of the Demulsification Efficiency of Some Ethoxylated Polyalkylphenol Formaldehydes Based on Locally Obtained Materials to Resolve Water-in-Oil Emulsions," *J DISPER SCI TECHNOL,* vol. 30, pp. 267-276, 2009.

[50] E. N. Stasiuk and L. L. Schramm, "The Influence of Solvent and Demulsifier Additions on Nascent Froth Formation during Flotation Recovery of Bitumen from Athabasca Oil Sands," *Fuel Processing Technology,* vol. 73, pp. 95-110, 2001.

[51] J. C. Pereira, J. Delgado-Linares, C. Scorzza, M. Rondon, S. Rodriguez and J.-L. Salager, "Breaking of Water-in-Crude Oil Emulsions. 4. Estimation of the Demulsifier Surfactant Performance to Destabilize the Asphaltenes Effect," *Energy & Fuels,* vol. 25, pp. 1045-1050, 2011.

[52] Y. Xu, J. Wu, T. Dabros and H. Hamza, "Effect of Demulsifier Properties on

Demulsification of Water-in-Oil Emulsion," *Energy & Fuels,* vol. 17, pp. 1554-1559, 2003.

[53] X. Feng, P. Mussone, S. Gao, S. Wang, S.-Y. Wu, J. Masliyah and Z. Xu, "Mechanistic Study on Demulsification of Water-in-Diluted Bitumen Emulsions by Ethylcellulose," *Langmuir,* vol. 26, pp. 3050-3057, 2010.

[54] P. M. Spiecker and P. K. Kilpatrick, "Interfacial Rheology of Petroleum Asphaltenes at the Oil-Water Interface," *Langmuir,* vol. 20, pp. 4022-4032, 2004.

[55] M. K. Krawczyk, D. T. Wasan and C. Shetty, "Chemical Demulsification of Petroleum Emulsions Using Oil-Soluble Demulsifiers," *Ind. Eng. Chem. Res,* vol. 30, pp. 367-375, 1991.

[56] C. Shetty, A. Nikolov and D. Wasan, "Demulsification of Water-in-Oil Emulsions Using Water Soluble Demulsifiers," *J. Dispersion Sci Technol,* vol. 13, pp. 121-133, 1992.

[57] X. Feng, Z. Xu and J. Masliyah, "Biodegradable Polymer for Demulsification of Water-in-Bitumen Emulsions," *Energy & Fuels,* vol. 23, pp. 451-465, 2009.

[58] I. Kailey, C. Blackwell and B. Jacqueline, "Effects of Crosslinking in Demulsification on Their Performance," *Can. J. Chem. Eng.,* vol. 91, pp. 1433-1438, 2013.

[59] U. G. Romanova, H. W. Yarranton, L. L. Schramm and W. E. Shelfantook, "Investigation of Oil Sands Froth Treatment," *The Canadian Journal of Chemical Engineering,* vol. 82, pp. 710-721, 2004.

[60] F. Seyer and C. Gyte, "Viscosity," in *AORTRA Technical Publication Series #6*, Edmonton, 1989, pp. 153-183.

[61] P. Tchoukov, J. Czarnecki and T. Dabros, "Study of Water-in-Oil Thin Films: Implications for the Stability of Petroleum Emulsions," *Colloids and Surfaces A: Physicochem. Eng. Aspects,* vol. 372, pp. 15-21, 2010.

[62] G. MacKay and S. Mason, "The Gravity Approach and Coalescence," *Can. J. Chem. Eng,* vol. 41, pp. 203-212, 1963.

[63] B. Steinhaus, P. T. Spicer and A. Q. Shen, "Droplet Size Effect on Film Drainage between Droplet and Subtrate," *Langmuir,* vol. 22, pp. 5308-5313, 2006.

[64] C. Guo, L. Jia, L. Yang, J. Xiang, Y. Tang and H. Liu, "Mechanism of PEO-PPO-PEO Micellization in Aqueous Solutions Studied by Two-dimensional Correction FTIR Spectroscopy," *Journal of Colloid and Interface Science,* vol. 345, pp. 332-337, 2010.

[65] C. Guo, J. Wang, H. Liu and J. Chen, "Hydration and Conformation of Temperature-Dependent Micellization of PEO-PPO-PEO Block Copolymers in Aqueous Solutions by FT-Raman," *Langmuir,* vol. 15, pp. 2703-2708,

1999.

[66] J. Kříž and J. Dybal, "Cooperative Preassociation Stages of PEO-PPO-PEO Triblock Copolymers: NMR, and Theoritical Study," *J. Phys. Chem. B,* vol. 114, pp. 3140-3151, 2010.

[67] G. D'Errico, L. Paduano, O. Ortona and G. Mangiapia, "Temperature and Concentration Effects on Supramolecular Aggregation and Phase Behavior for Poly(propylene oxide)-Poly(ethylene oxide)-Poly(propylene oxide) Copolymers of Different Concentration in Aqueous Mixtures, 2," *Journal of Colloidal and Interface Science,* vol. 359, pp. 179-188, 2011.

[68] J. Ma, Y. Wang, C. Guo, H. Liu, Y. Tang and P. Bahadur, "Oil-Induced Aggregation of Block Copolymer in Aqueous Solutions," *J. Phys. Chem B,* vol. 111, pp. 11140-11148, 2007.

[69] V. Mishra, S. M. Kresta and J. H. Masliyah, "Self-Preservation of the Drop Size Distribution Function and Variation in the Stability Ratio for Rapid Coalescence of a Polydisperse Emulsion in a Simple Shear Field," *Journal of Colloid and Interface Science,* vol. 197, pp. 57-67, 1998.

[70] S. Dukhin, O. Soether and J. Sjoblom, "Coupling of Coalescence and Flocculation in Dilute O/W Emulsions," in *Encyclopedic Handbook of Emulsion Technology*, Basel, Marcel Dekker, Inc., 2001, pp. 71-92.

[71] T. Krebs, K. Schroen and R. Boom, "A Microfluidic Method to Study

Demulsification Kinitics," *Lab on a Chip,* vol. 12, pp. 1060-1070, 2012.

[72] B. Singh, "Correlation Between Surface Film Pressure and Stability of Emulsion," *Energy Sources,* vol. 19, pp. 783-788, 1997.

[73] G. Hou, G. Power, M. Barrett, B. Glennon, G. Morris and Y. Zhao, "Development and Characterization of A Single Stage Mixed-Suspension, Mixed-Product-Removal Crystallization Process with A Novel Transfer Unit," *Crystal Growth and Design,* vol. 14, pp. 1782-1793, 2014.

[74] Y. Qian, G. Lu, Y. Sun, X. Song and J. Yu, "Metastable zone width of SrCl2·6H2O during cooling crystallization," *Crystal Research and Technology,* vol. 2014, pp. 78-83, 2014.

[75] D. J. Turner, K. T. Miller and E. D. Sloan, "Direct Coversion of Water Droplets to Methane Hydrate in Crude Oil," *Chemical Engineering Science,* vol. 64, pp. 5066-5072, 209.

[76] H. Liu, L. Mu, B. Wang, B. Liu, J. Wang, X. Zhang, C. Sun, J. Chen, M. Jia and G. Chen, "Separation of Ethylene from Refinery Dry Gas via Forming Hydrate in W/O Dispersion System," *Separation and Purification Technology,* vol. 116, pp. 342-350, 2013.

[77] J. Marugan, J. A. Calles, J. Dufour, R. Gimenez-Aguirre, J. L. Pena and D. Merino-Garcia, "Characterization of the Asphaltene Onset Region by Focused-Beam Laser Reflectance: A Tool for Additives Screening," *Energy*

& Fuels, vol. 23, pp. 1155-1161, 2009.

[78] D. Greaves, J. Boxal, J. Mulligan, A. Montesi, J. Creek and D. E. Sloan, "Measureing the Particle Size of a Known Distribution Using the Focused Beam Reflectance Measurement Technique," *Chemical Engineering Science,* vol. 63, pp. 5410-5419, 2008.

[79] M. Toledo, "Lasentec FBRM S400 Hardware Manual," 2007.

[80] C. R. Mansur, F. C. Lechuga, A. C. Mauro, G. Gonzalez and E. F. Lucas, "Behavior of Mixtures of Nonionice Polyoxide-Based Surfactants & TheirApplication in the Destabilization of Oil Emulsions," *J APPL POLYM SCI,* vol. 106, pp. 2947-2954, 2007.

[81] A. M. Atta, A. A. Fadda, A. A.-H. Abdel-Rahman, H. S. Ismail and R. R. Fouad, "Application of New Modified Poly(ethylene oxide)-Block-Poly(propylene oxide)-Block-Poly(ethylene oxide) Copolymers as Demulsifier for Petroleum Crude Oil Emulsions," *J. Dispersion Sci Tech,* vol. 33, pp. 775-785, 2011.

[82] I. Kailey and X. Feng, "Influence of Structural Variations of Demulsifiers on their Performance," *Ind. Eng. Chem. Res.,* vol. 52, pp. 758-793, 2013.

[83] J. K. Ferri and K. J. Stebe, "Which Surfactants Reduce Surface Tension Faster? A Scaling Argument for Diffusion-Controlled Adsorption," *Advances in Colloid and Interface Science,* vol. 85, pp. 61-97, 2000.

[84] R. Prokop, M. Hair and A. Neumann, "Interfacial Tension of a Polystyrene-Poly(ethylene oxide) Diblock Copolymer at the Water-Toluene Interface," *Macromolecules,* vol. 29, pp. 5902-5906, 1996.

[85] A. A. Pena, G. J. Hiraski and C. A. Miller, "Chemically Induced Destabilization of Water-in-Crude Oil Emulsions," *Ind. Eng. Chem. Res.,* vol. 44, pp. 1139-1148, 2005.

[86] S. Wang, E. Axcell, R. Bosch and V. Little, "Effects of Chemical Application on Antifouling in Steam-Assisted Gravity Drainage Operations," *Energy and Fuels,* vol. 19, pp. 1425-1429, 2005.

[87] J. Wu, Y. Xu, T. Dabros, H. Hamza, S. Wang, M. Bidal, J. Venter and T. Tran, "Breaking Water-in-Bitumen Emulsions using Polyoxyalkylated DETA Demulsifier," *The Canadian Journal of Chemical Engineering,* vol. 82, pp. 829-835, 2004.

[88] Y. Fan, S. Simon and S. Johan, "Chemical Destabilization of Crude Oil Emulsions: Effect of Nonionic Surfactants as Emulsion Inhibitors," *Energy & Fuels,* vol. 23, pp. 4575-4583, 2009.

[89] C. S. Shetty, A. D. Nikolov, D. T. Wasan and B. R. Bhattacharyya, "Demulsification of Water in Oil Emulsions Using Water Soluble Demulsifiers," *J. Dispersion Sci. Technol.,* vol. 13, pp. 121-133, 1992.

[90] M.-H. Ese, . L. Galet and D. Claus, "Properties of Langmuir Surface and

Interfacial Films Built up by Asphaltenes and Resins: Influence of Chemical Demulsifiers," *J. Colloid Interface Sci,* vol. 220, pp. 293-301, 1999.

[91] N. N. Zaki, M. E. Abdel-Raouf and A.-A. A. Abdel-Azim, "Polyoxyethylenated Bisphenol-A for Breaking Water-in-Oil Emulsions," *Polymers for Advanced Technologies,* vol. 7, pp. 805-808, 1996.

[92] A. Bhardwaj and S. Hartland, "Study of Demulsification of Water-in-Crude Oil Emulsion," *Journal of Dispersion Science and Technology,* vol. 14, pp. 541-557, 1993.

Appendix

Calibration of the FBRM probe using silica particles in aqueous phase and diluted bitumen

The procedure and data provided in Appendix aim to illustrate the accuracy and characteristics of FBRM size measurement.

Silica particles used in the calibration were fine grounded silica particles purchased from US Silica™ (brand name: MIN-U-SIL). The maximum size of the silica particles was 5 μm.

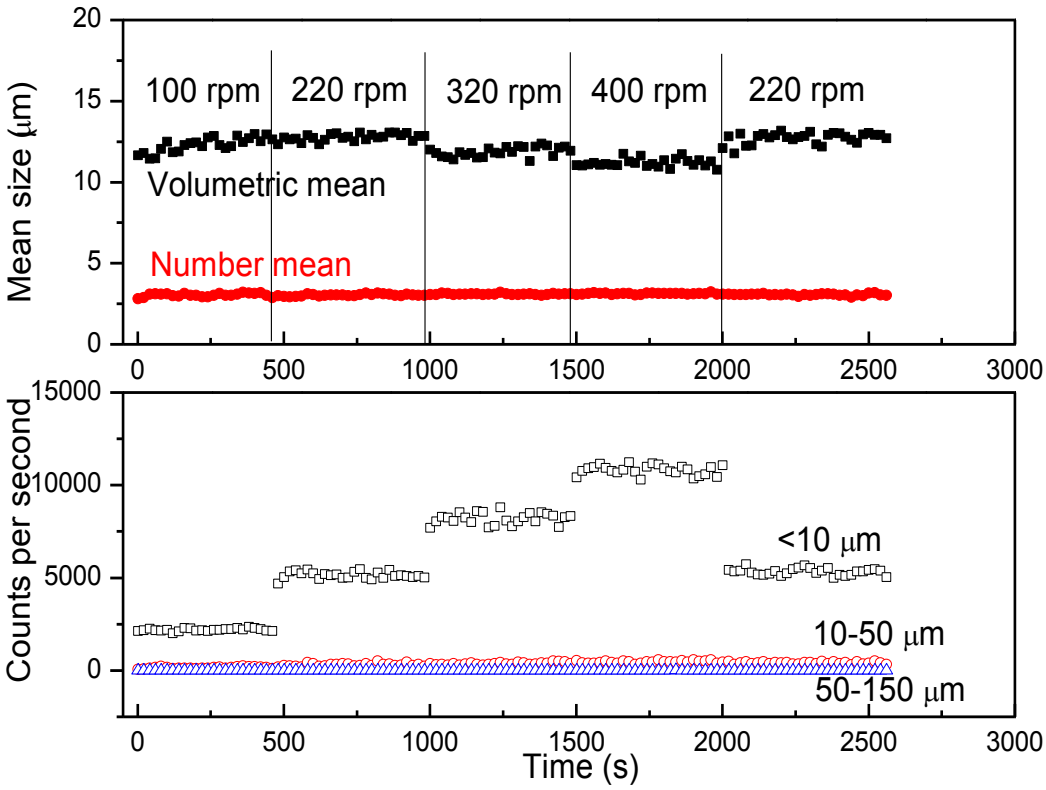

Appendix Figure 1. Size and counts of silica particles in aqueous phase measured by FBRM.

Appendix Figure 1 shows that the number mean of the silica particles was around 2.7 μm, where the volumetric mean size of the silica particles was around 12.5 μm. Varying the stirring speeds caused changes to silica particles counts. The increase in stirring speed increased the counts of the silica particles since more particles were allowed to be observed by the sapphire window of the FBRM probe in a given time.

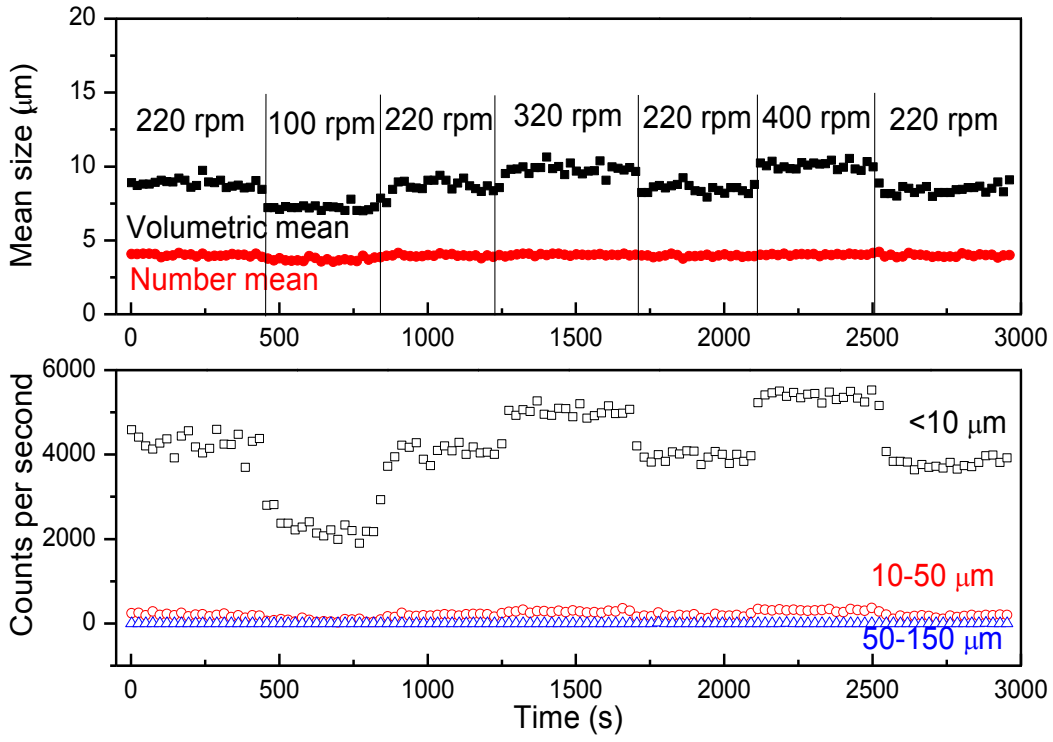

Appendix Figure 2. Size and counts of silica particles in diluted bitumen phase measured by FBRM.

Appendix Figure 2 shows the mean sizes and counts of the silica particles in the diluted bitumen suspension at 50 °C. The measurement was done at elevated temperature in order to keep the viscosity of the fluid at a relatively low level. The number mean of the system reported by the FBRM was about 3.8 μm, whereas

the volumetric mean was below 10 μm. The counts of silica particles at different stirring speeds show that the faster the particles moved, the more of them can be observed by the FBRM probe, which is the same as it observed in the case of silica in DI water suspension.

To understand the inconsistency of the mean sizes reported by the FBRM at the two conditions, the differences between the fluid media of the two cases need to be considered first. The silica particles tend to repel each other in an aqueous suspension whose pH is not at the Particle Zero Charge (PZC) point of silica as a result of electrical repelling from their surface charges. This explains why the number mean of the silica particles in the oil phase was larger than its value in DI water. The volumetric mean was influence not only by the sizes of particles but also their counts. Comparing the counts of silica particles with relatively large size, it is found that the counts per second of silica particles falling in 10 – 50 μm in diameter were between 300 – 500 in DI water, whereas the counts per second of silica particles in the same size range were 100 – 200 in the diluted bitumen. At a fixed stirring speed 220 rpm, the counts of small silica particles whose diameter is below 10 μm were very close for both cases. This explains the difference of volumetric mean size of the silica particles in the two suspensions.